

Review

Structure and Bonding in Planar Hypercoordinate Carbon Compounds

Prasenjit Das  and Pratim Kumar Chattaraj * 

Department of Chemistry, Indian Institute of Technology Kharagpur, Kharagpur 721302, India

* Correspondence: pkc@chem.iitkgp.ac.in

Abstract: The term hypercoordination refers to the extent of the coordination of an element by its normal value. In the hypercoordination sphere, the element can achieve planar and/or non-planar molecular shape. Hence, planar hypercoordinate carbon species violate two structural rules: (i) The highest coordination number of carbon is four and (ii) the tetrahedral orientation by the connected elements and/or groups. The unusual planar orientations are mostly stabilized by the electronic interactions of the central atom with the surrounding ligands. In this review article, we will talk about the current progress in the theoretical prediction of viable planar hypercoordinate carbon compounds. Primary knowledge of the planar hypercoordinate chemistry will lead to its forthcoming expansion. Experimental and theoretical interests in planar tetracoordinate carbon (ptC), planar pentacoordinate carbon (ppC), and planar hexacoordinate carbon (phC) are continued. The proposed electronic and mechanical strategies are helpful for the designing of the ptC compounds. Moreover, the 18-valence electron rule can guide the design of new ptC clusters computationally as well as experimentally. However, the counting of 18-valence electrons is not a requisite condition to contain a ptC in a cluster. Furthermore, this ptC idea is expanded to the probability of a greater coordination number of carbon in planar orientations. Unfortunately, until now, there are no such logical approaches to designing ppC, phC, or higher-coordinate carbon molecules/ions. There exist a few global minimum structures of phC clusters identified computationally, but none have been detected experimentally. All planar hypercoordinate carbon species in the global minima may be feasible in the gas phase.

Keywords: anti-van't Hoff Le Bel; planar tetracoordinate carbon; planar pentacoordinate carbon; planar hexacoordinate carbon; σ/π -dual aromaticity



Citation: Das, P.; Chattaraj, P.K. Structure and Bonding in Planar Hypercoordinate Carbon Compounds. *Chemistry* **2022**, *4*, 1723–1756. <https://doi.org/10.3390/chemistry4040113>

Academic Editor: Venkatesan S. Thimmakonda

Received: 4 November 2022

Accepted: 13 December 2022

Published: 15 December 2022

Publisher's Note: MDPI stays neutral with regard to jurisdictional claims in published maps and institutional affiliations.



Copyright: © 2022 by the authors. Licensee MDPI, Basel, Switzerland. This article is an open access article distributed under the terms and conditions of the Creative Commons Attribution (CC BY) license (<https://creativecommons.org/licenses/by/4.0/>).

1. Introduction

The systems containing planar tetracoordinate carbons are seminal examples of non-classical species [1–7]. The non-classical species have outstanding optical, magnetic, and electronic characteristics and have various potential applications. Most organic molecules are based on two structural rules, (i) the highest coordination number of carbon is four and (ii) the tetrahedral orientation by the connected elements and/or groups [3,8]. However, at that time, it was not considered that the tetracoordinate tetrahedral carbon (ttC) model is valid up to what extent. Therefore, without knowing the beautiful ptC concept, many molecules were characterized. In 1968, the idea of ptC was established by H. J. Monkhurst as a transition state structure of methane in a non-dissociative racemization process [9]. This concept was introduced in the work of Professor Hans Wynberg whose group synthesized the $CR_1R_2R_3R_4$ hydrocarbons with four non-identical alkyl groups (R_1 , R_2 , R_3 , and R_4) by the chiral routes but did not obtain measurable optical activity [10]. Then, to determine the energy barrier for the possibilities of thermal racemization that causes no optical activity, Professor H. J. Monkhurst began theoretical calculations and ruled out the possibility of planar methane due to its very high relative energy. His intention was not to determine a ptC minimum but rather to conclude that the stereo mutation of methane via a ptC intermediate is quite unfeasible. Later, Roald Hoffmann and co-workers started to explore

“how to stabilize a planar geometry so that it could serve as a thermally accessible transition state for a classical racemization experiment” to determine a strategy to lower the ptC stereo mutation energy barriers. They concluded that “it would seem too much to hope for a simple carbon compound to prefer a planar to a tetrahedral structure”. Their 1970 breakthrough was the perspicacious analysis of ptC bonding in a speculative planar CH₄ molecule [11]. Their electronic approach to stabilize ptCs suggested that the σ -donating ligands give electrons to central carbon and, simultaneously, the π -accepting behavior of the ligands takes the lone pair on the carbon atom.

In this review article, we cover the recent advancement in planar hypercoordinate carbon chemistry. Various examples of planar tetracoordinate, pentacoordinate, hexacoordinate, and heptacoordinate molecules, ions, and clusters are included in this article. Some experimentally characterized planar species are also discussed in this article. The electronic and mechanical approaches that are utilized to generate ptCs are discussed. We hope that this review article with various examples will give a primary understanding of planar hypercoordinate carbon, which will lead to its forthcoming expansion.

2. Planar Tetracoordinate Carbons (ptCs)

2.1. How to Achieve ptCs

Methane (CH₄) is the simplest hypothetical ptC molecule to think about. The hybridization changes from sp³ to sp² for the planar D_{4h} configuration. The planar configuration is approximately 130 kcal mol⁻¹ higher in energy compared to the lowest-energy tetrahedral geometry [12]. Even the planar structure has higher energy than the C–H bond detachment energy (103 kcal mol⁻¹) [13]. After the analysis of the electronic structure of the planar CH₄ molecule, Hoffmann and co-workers suggested a way to stabilize the planar structures. When the tetrahedral structure of methane becomes planar, an extra lone pair is available on the central carbon, which distorts its planar geometry. The other point is the electron-deficient nature of the C–H bonds in the planar form. They suggested that the replacement of hydrogens by σ -donor ligands overcome the electron deficiency problem of the C–H bonds, as the ligands give electrons to the carbon atom. The ligands should have π -acceptor capacity so that they can accept the lone pair on the carbon. So, with the incorporation of simultaneous σ -donor and π -acceptor ligands, a ptC structure can be generated, and this strategy is called the “*electronic approach*”. Using this approach, many ptC molecules have been theoretically reported [14–31] and experimentally characterized [32–40].

In addition to the electronic approach, ptC structures can be designed by generating enough strain to keep the carbon forcefully in planar orientations, and this method is called the “*mechanical strategy*”. In this particular approach, to generate sufficient strain, cylindrical cages or tubes, small rings, and annulenes are helpful agents [41–47]. Although some species with ptC were designed theoretically by using this strategy, no experimentally characterized ptC structures based on this strategy have been reported. Following this strategy, some of the computationally predicted ptC species are shown in Figure 1. To achieve ptC structures based on this approach, the fenestrenes and the aromatic unsaturated fenestrenes, rigid 3D cages, such as octaplane, were proposed initially [48,49]. In 1999, Ding et al. noted that “*despite considerable computational efforts no structures with a planar tetracoordinate C(C)₄ substructure have been found*” [50]. However, Rasmussen et al. computationally reported the first successful ptC structure based on this strategy by adjusting the **1g** structure to generate **1h** (Figure 1) geometry in which the ptC atom is stabilized in a strained environment [44,51]. With the use of a similar strategy, Wang and Schleyer reported a set of boron spiroalkanes with a planar C(C)₄ moiety through the replacement of carbon by boron atoms [20,52].

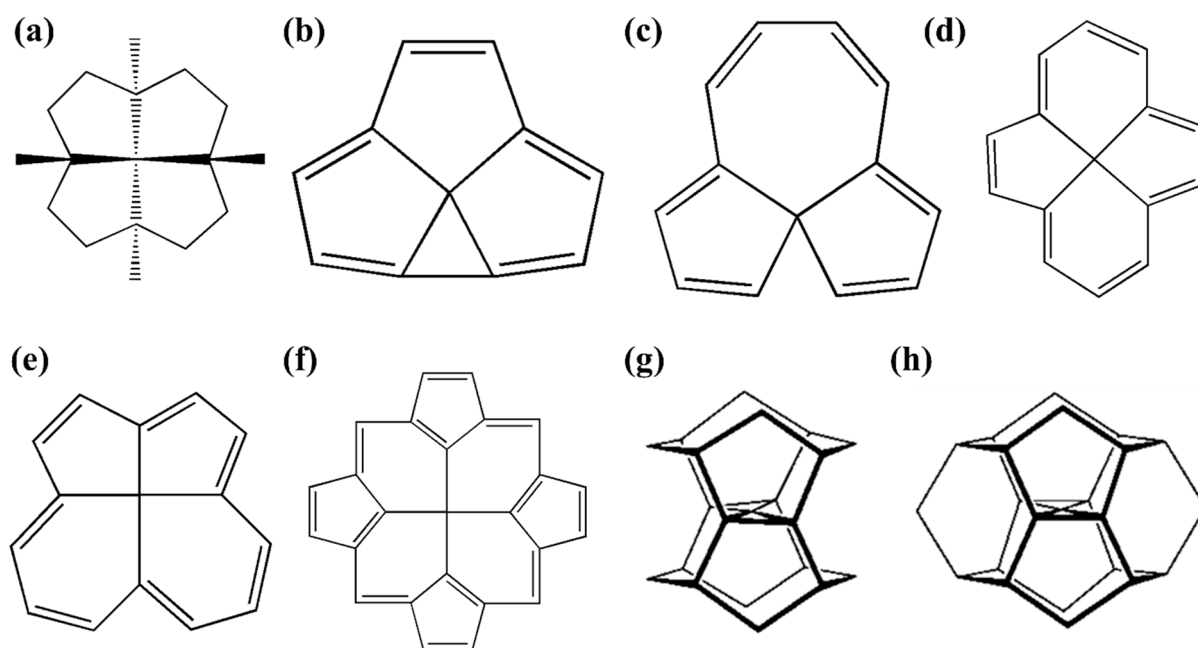


Figure 1. Schematic presentations of various mechanically stabilized ptC molecules (a–h).

2.2. Early Examples of ptCs

With the help of the two suggested strategies, the first example of ptC came from Collins et al. in 1976 [53]. Through a systematic computational investigation, they reported 1,1-dilithiocyclopropane (Figure 2a) and 3,3-dilithiocyclopropene (Figure 2b) systems with ptCs in the energy minimum geometries and the tetrahedral orientations have higher energies than the corresponding planar configurations. One year later, the first experimentally characterized ptC containing compound $V_2(2,6\text{-dimethoxyphenyl})_4$ (Figure 2c) was published by Cotton et al. [54]. This complex contains triple bonds between two vanadium (V) centers and has two ptCs at two ligand rings. However, unfortunately, at that time, the original authors did not realize this beautiful fact. This system has importance in this background as it is the first experimentally predicted ptC-containing compound. Due to the ionic bonding nature of lithium (Li), it prefers bridging positions, and with this concept, Xie et al. in 1991 designed a D_{6h} symmetric C_6Li_6 system with ptCs (Figure 2d) [55]. The simplest molecule with a ptC has only five atoms, and the first example of this category was CA_2Si_2 , which was reported in 1991 by Schleyer and Boldyrev [15]. They concluded that *cis* and *trans* isomers of CSi_2Al_2 (Figure 3a and 3b, respectively) were local minimum geometries with a ptC, but they did not mention the energy of the tetrahedral-like geometry of this system. They first introduced the 18-valence electron counting concept for the stabilization of planar geometries. After seven years, in 1998, Boldyrev and Simons computed the energies of the planar and tetrahedral-like geometries of the CSi_2Al_2 system, and then they expanded the search for the possibility of a ptC atom in higher analogues such as CSi_2Ga_2 and CGe_2Al_2 species in order to determine the size dependency of the surrounding atoms on the stabilities of these species in planar orientations [16]. The optimized structures of CSi_2Al_2 in singlet states are given in Figure 3. The *cis* and *trans* isomers of the CSi_2Al_2 system are energy minima based on the theoretical analysis using the B3LYP/6-311+G* method, which is in agreement with the earlier conclusion at the MP2/6-31G* level of theory. However, both these isomers become saddle points in the MP2(full)/6-31+G* and MP2(full)/6-311+G* methods [16]. The authors reported that in the case of the CSi_2Al_2 system, the tetrahedral-type geometry is a first-order saddle point in the B3LYP/6-311+G* and MP2(full)/6-311+G* methods and has almost 27–28 kcal mol⁻¹ higher energy than the more stable quasi planar *cis* and *trans* isomers 3a and 3b, respectively (Figure 3) [16]. Then they studied two 18-valence isoelectronic species, CSi_2Ga_2 and CGe_2Al_2 , where the cavities

for the carbon center happened to be larger than that in the CSi_2Al_2 system. However, this time they only optimized planar *cis* and *trans* and tetrahedral geometries for CSi_2Ga_2 and CGe_2Al_2 systems. In the B3LYP/6-311+G* and MP2(fc)/6-311+G* methods, the planar *cis* and *trans* isomers of both these species were reported as energy minima [16]. However, the *cis* isomer (Figure 3c) of CSi_2Ga_2 is less stable than the *trans* isomer (Figure 3d) by 2 kcal mol⁻¹, while, for the CGe_2Al_2 system, the *cis* isomer (Figure 3e) has 3 kcal mol⁻¹ lower energy than the *trans* isomer (Figure 3f). They also reported that the tetrahedral-type geometries have 27 and 25 kcal mol⁻¹ more energy than the most stable isomers for CSi_2Ga_2 and CGe_2Al_2 systems, respectively. The increase in the size of the cavity in the CSi_2Ga_2 and CGe_2Al_2 species permits the incorporation of carbon into it and thus maintains the planar structures. From these analyses, they concluded that pentatomic species with a carbon center and two Al or Ga and two Si or Ge surrounding atoms should have stable planar geometries [16]. The planar structures may be preferred over the tetrahedral one when Jahn–Teller distortion makes the tetrahedral geometries unstable and the formation of the maximal carbon–ligand and ligand–ligand bonding by the valence electrons. For this purpose, they compared the occupancy pattern of the valence molecular orbitals (MOs) of the tetrahedral CF_4 molecule with the tetrahedral structures of their systems. The CF_4 molecule is a 32-valence electronic system, and the occupancy pattern of the occupied MOs is $1a_1^2 1t_2^6 2a_1^2 2t_2^6 1e^4 3t_2^6 1t_1^6$. They assumed other tetrahedral molecules or nearly tetrahedral structures will follow this occupancy pattern (except for symmetry-imposed degeneracies) and the 18-valence electronic tetrahedral structures show $1a_1^2 1t_2^6 2a_1^2 2t_2^6 1e^2$ pattern of occupancy. Due to this partially filled e-orbital, the tetrahedral structures of their systems show Jahn–Teller instability and become distorted to a planar structure. They suggested that the presence of 18-valence electrons is crucial for planar geometries to be stable and preferred over tetrahedral structures. The formation of three σ and one π bonds among the middle carbon and the surrounding atoms and one ligand–ligand bond are the consequences of 18-valence electrons, the appeasement case for planar geometries. It took a long time to encourage experimental researchers to test this prognosis. Nevertheless, the species CAL_4^- and CAL_3Si^- (isoelectronic to CSi_2Ga_2) were prepared in molecular beams and the planarity of these systems was experimentally confirmed [18,40,56].

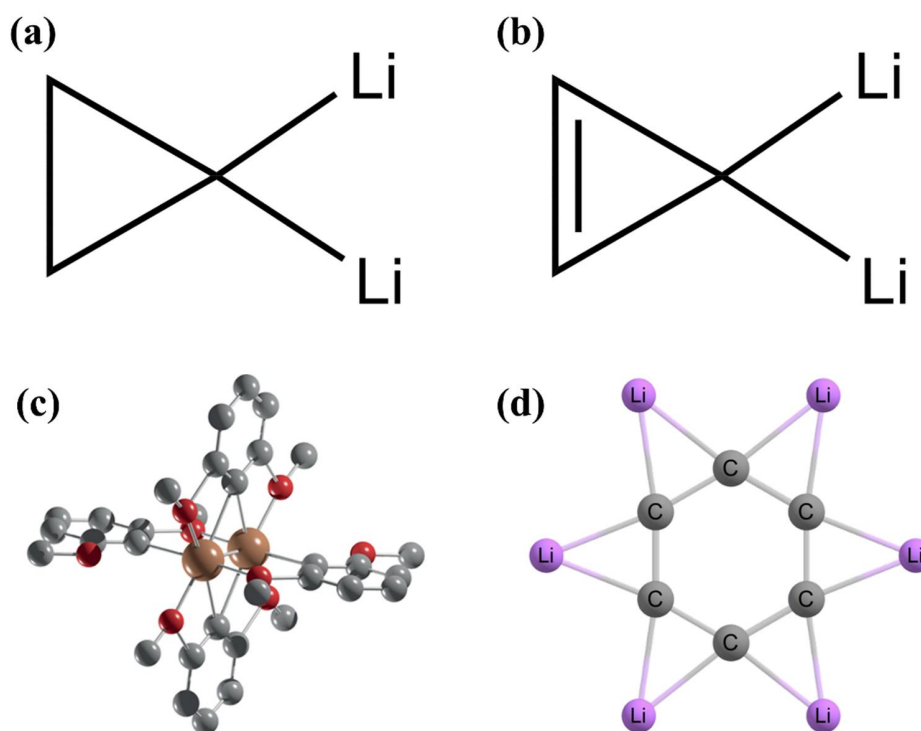


Figure 2. Optimized geometries of (a) 1,1-dilithiocyclopropane and (b) 3,3-dilithiocyclopropene

systems. (c) The molecular structure of $V_2(2,6\text{-dimethoxyphenyl})_4$ features a $V\equiv V$ triple bond and two planar tetracoordinate carbon (ptC) centers. The H atoms are omitted for clarity. (d) Optimized D_{6h} symmetric structure of C_6Li_6 .

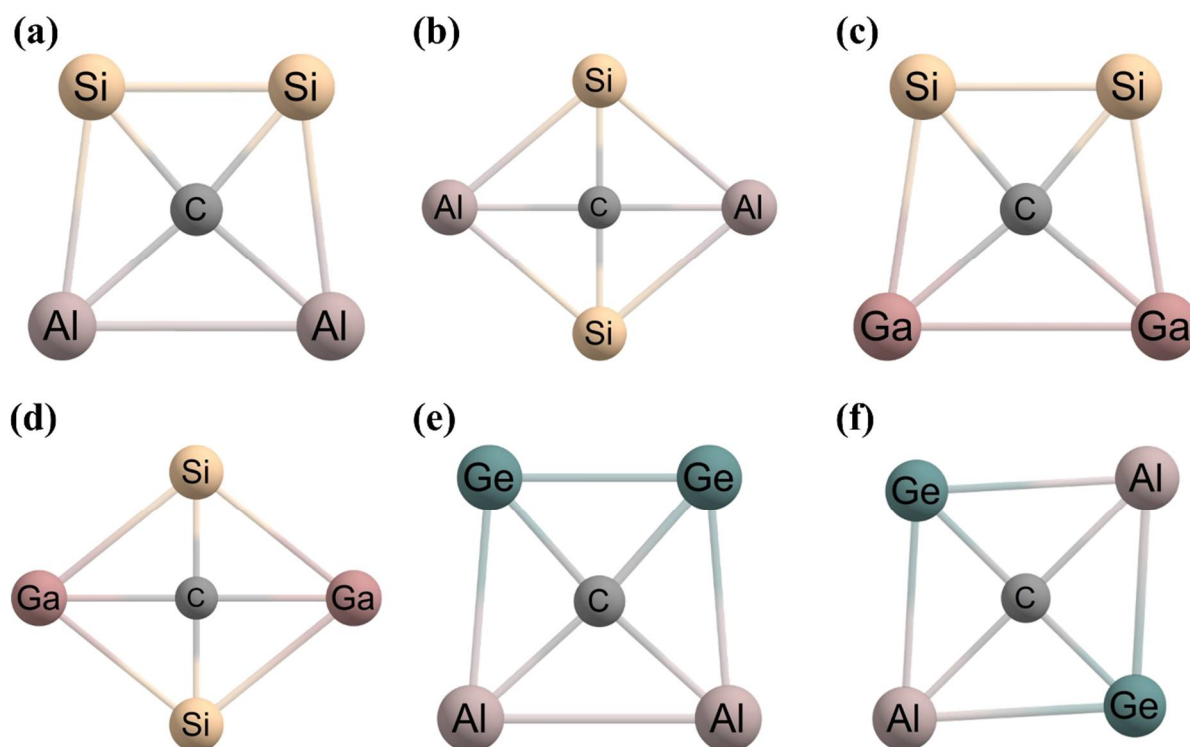


Figure 3. Optimized geometries of (a) *cis*- CSi_2Al_2 , (b) *trans*- CSi_2Al_2 , (c) *cis*- CSi_2Ga_2 , (d) *trans*- CSi_2Ga_2 , (e) *cis*- CGe_2Al_2 , and (f) *trans*- CGe_2Al_2 systems. Structure (a) has $1.16 \text{ kcal mol}^{-1}$ lower energy than structure (b). Structure (c) has $2.01 \text{ kcal mol}^{-1}$ higher energy than structure (d). Structure (e) has $2.87 \text{ kcal mol}^{-1}$ lower energy than structure (f).

With the use of Li as ligand atoms, a series of ptC species can be adapted [19]. For example, the replacement of the CH_2 group in the 1,1-dilithiocyclopropane (Figure 2a) molecule by isoelectronic NH and O generates ptC structures **4a** and **4b**, respectively (Figure 4). The **4c** and **4d** ptC structures are also generated by attaching **4a** to a heterocyclic system and a benzene ring, respectively. These **4c** and **4d** species are more viable targets due to the dominance of the aromaticity of imidazole.

2.3. Recent Examples of ptCs with 18 Valence Electrons

In 2012, Castro et al. designed CE_4^{2-} ($E = Al-Tl$) clusters (Figure 4e) with a ptC center in the lowest energy structures [57]. For all the clusters, the other two low-lying isomers have over 20 kcal mol^{-1} more energy than the ptC isomer. The natural charge analysis shows that the central carbon acts as a simultaneous σ -acceptor and π -donor. The σ -acceptor is confirmed by the high charge density on the carbon atom. The higher occupancies of $2p_x$ and $2p_y$ as compared to the $2p_z$ orbitals are the revelation of the π -back-donation. The authors neutralized one negative charge of the clusters by one Li^+ ion and the systems are CE_4Li^- ($E = Al-Tl$) [57]. The binding of the Li^+ ion to the di-anionic system does not significantly disrupt the ptC core. For the CaL_4Li^- and CGa_4Li^- clusters, the lowest-energy geometries are planar in which the Li^+ ion bridges the two Al and Ga atoms, respectively (Figure 5). Moreover, the pyramidal geometries of CaL_4Li^- and CGa_4Li^- clusters are 11.2 and $6.3 \text{ kcal mol}^{-1}$ higher in energy as compared to the lowest-energy isomers, respectively. However, in the case of the CIn_4Li^- and CTl_4Li^- clusters, the 3D geometries with C_{4v} symmetry are the lowest-energy structures (Figure 5). The planar

structures have 2.5 and 6.8 kcal mol⁻¹ higher energy than the pyramidal geometries for CIn₄Li⁻ and CTl₄Li⁻ clusters, respectively [57].

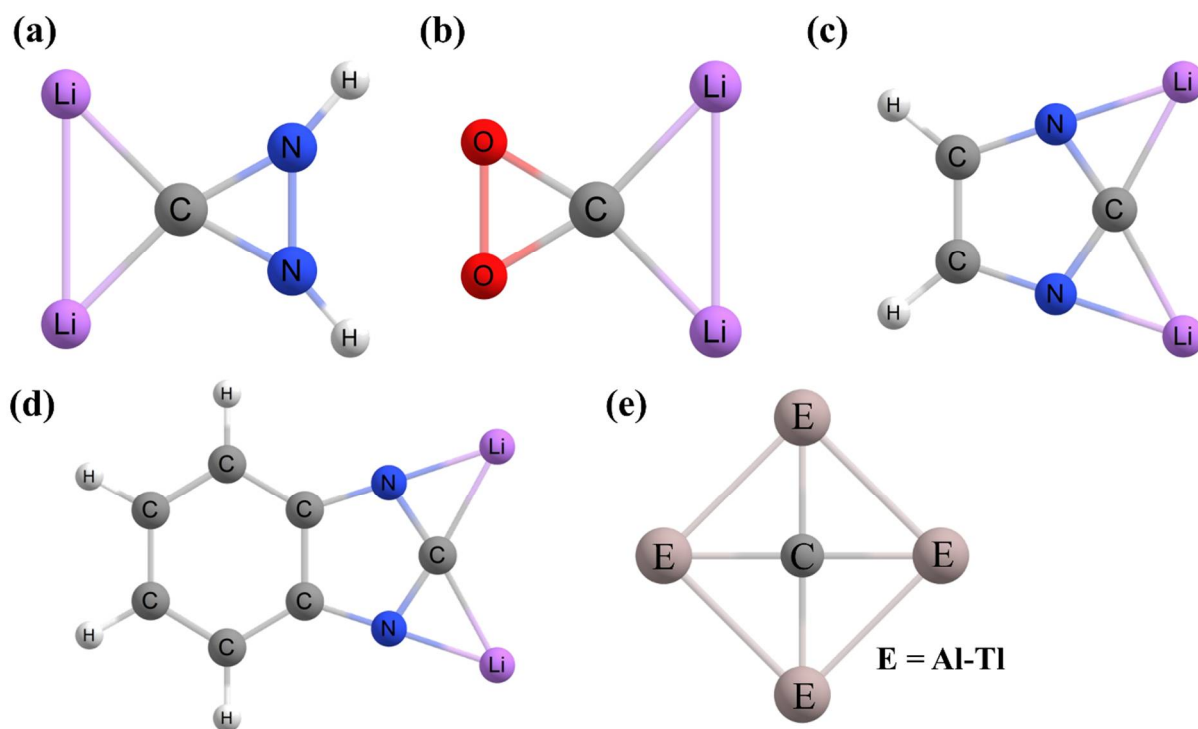


Figure 4. Optimized geometries of (a–d) computationally predicted dilithium ptC compounds. (e) The lowest energy structures of CE₄²⁻ clusters (E = Al, Ga, In, Tl), the systems have the same shape but different bond lengths.

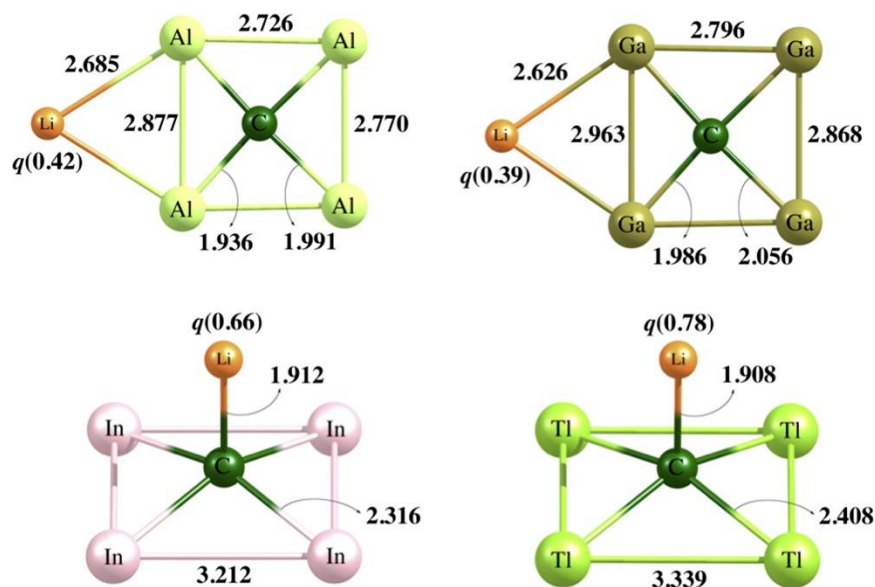


Figure 5. Lowest-energy structures of the CE₄Li⁻ clusters (E = Al, Ga, In, Tl), respectively, calculated at the B3LYP/def2-TZVP level. Bond lengths are given in Å. (Reprinted from ref. [57] with permission from Elsevier. Copyright © 2022 Elsevier B.V.).

Merino and coworkers reported the presence of a ptC center in the global minimum geometries of the neutral and 18-valence electronic CA₃E (E = P, As, Sb, Bi) clusters (Figure 6a) [58]. The closest competitive isomer for all the clusters is more than 14 kcal

mol^{-1} higher energy than the ptC isomers. The energy gap between the highest occupied molecular orbital (HOMO) and the lowest unoccupied molecular orbital (LUMO) decreases drastically from P to Bi, indicating a decrease in the stability following the maximum hardness principle (MHP) [59–61]. In these clusters, the π -bonding orbital is mainly located on the C–E bonds unlike the other ptC clusters, and this bond is classified as a double bond. The existence of the C=E bonds is confirmed by the Wiberg bond index (WBI) values [62] and the adaptive natural density partitioning (AdNDP) [63,64] analysis. Additionally, the WBI values for C=E bonds decrease moderately from P to Bi, indicating that the inclusion of the heavier elements causes a decrease in the ability to form C=E bonds. For the CAI_3P and CAI_3As clusters, a remarkable electron shift occurs from the Al atoms to the central carbon. However, in the case of the CAI_3Sb and CAI_3Bi clusters, the electron shift from E and Al atoms to the central carbon is competitive. Simultaneously, the ptC center acts as the π -donor in the clusters. The ptC global minima are kinetically stable enough as predicted by the Born–Oppenheimer molecular dynamics (BOMD) [65] simulations at temperatures of 323 K and 373 K.

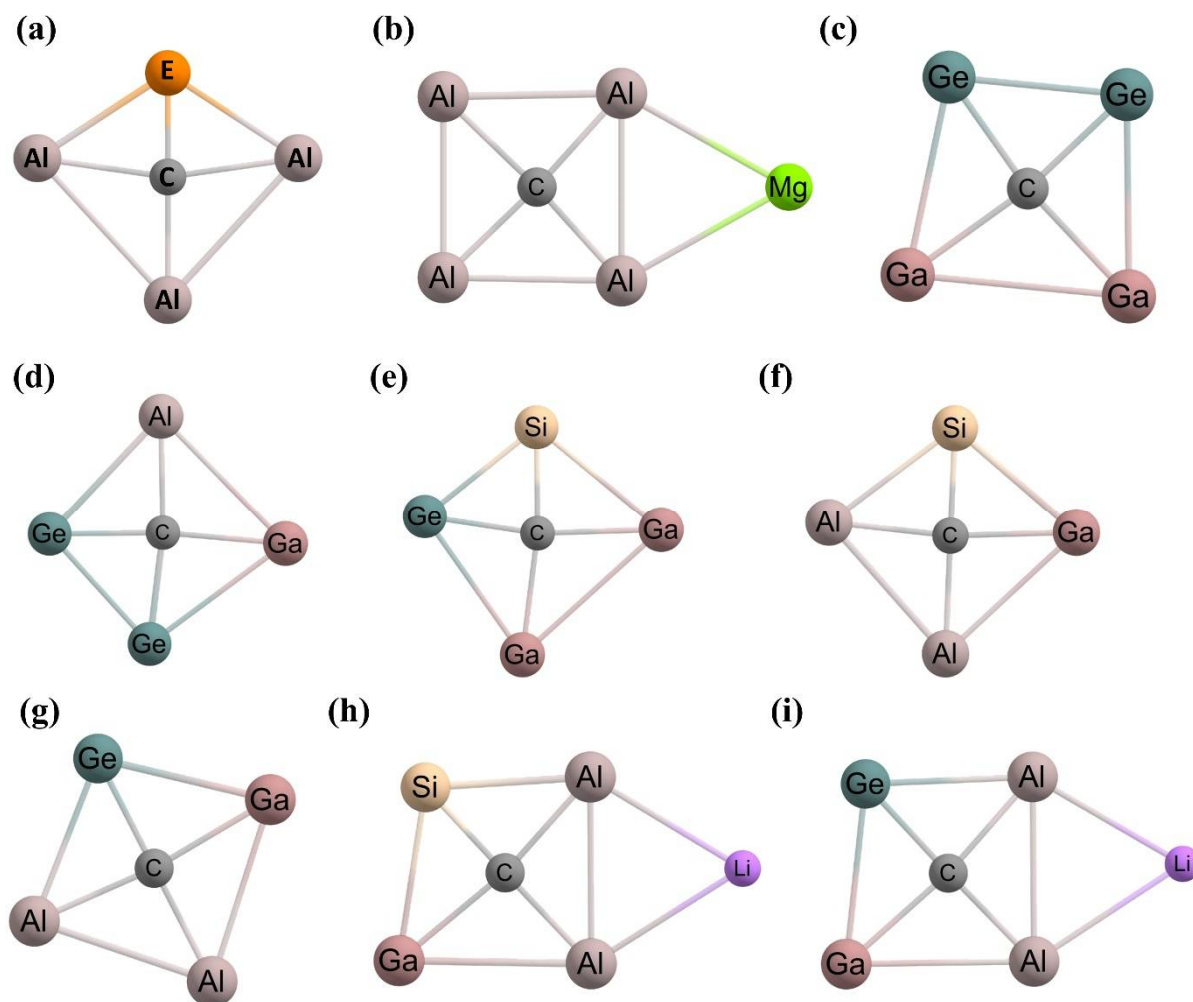


Figure 6. (a) Global minimum structures of the CAI_3E ($\text{E} = \text{P}, \text{As}, \text{Sb}, \text{Bi}$) clusters. (b) The global minimum structures of CAI_4Mg and CAI_4Mg^- clusters. The neutral and anionic forms have the same shape but different bond lengths. The minimum energy structures of (c) CGa_2Ge_2 , (d) CAIGaGe_2 , (e) CSiGa_2Ge , (f) CSiGaAl_2^- , (g) CGeGaAl_2^- , (h) Li@SiGaAl_2 , and (i) Li@GeGaAl_2 clusters.

Job et al. in 2021 designed an 18-valence electronic CAI_4Mg cluster with a ptC atom in the global minimum energy structure with C_{2v} symmetry (Figure 6b) [66]. The second-lowest-energy isomer lies at $2.63 \text{ kcal mol}^{-1}$ above the ptC isomer. The ptC structure

exhibits σ/π double aromaticity as determined by the nucleus-independent chemical shift (NICS) [67–70] calculations. The atom-centered density matrix propagation (ADMP) [71–75] simulation at 298 K for 10 ps confirmed the dynamical stability of the ptC isomer. The natural charge analysis showed that the central carbon atom acts as a simultaneous σ -acceptor and π -donor. Electron delocalization within the ptC fragment is well understood from the molecular orbitals, electron localization function (ELF) [76,77], and AdNDP analyses.

Recently, we reported three pentatomic neutral CGa_2Ge_2 , CAIgaGe_2 , and CSiGa_2Ge (Figure 6c to 6e, respectively) molecules with 18-valence electrons that show a ptC in the minimum-energy structure [78]. The ADMP simulations at 300 K and 500 K show the dynamic stability of the clusters. The natural charge calculations predicted that in all the systems, there is a significant charge transfer (σ -donation) from the surrounding atoms to the middle carbon, and, simultaneously, π -back donation from the carbon to the ligand atoms is also verified. The NICS computations show the σ/π -dual aromaticity of the ptC geometries. The AdNDP analysis shows the $2\pi/6\sigma$ framework of the ptC core in all the systems, which is crucial to maintain the planarity.

Another most recent work from our group predicted that the mono-anionic 18-valence electronic CSiGaAl_2^- and CGeGaAl_2^- clusters (Figure 6f and 6g, respectively) have a ptC in the global minimum geometries [79]. The closest competitive isomers for both clusters are more than $8.0 \text{ kcal mol}^{-1}$ higher energy as compared to the ptC isomers. The ptC structures are dynamically stable at 300 K and 500 K temperatures. The simultaneous σ -donation from the surrounding atoms to the carbon and the π -acceptance of the peripheral atoms from the central carbon fulfilled the criteria of the electronic approach to stabilize ptC clusters. The systems are σ/π -dual aromatic. The molecular orbitals along with associated energies for the ptC isomers of both systems are given in Figure 7. In both cases, the HOMO-4 exhibits π -delocalization and HOMO-5 shows the σ -delocalization within the whole clusters. In the HOMO-4 π -delocalized MO of the systems, a significant contribution comes from the perpendicular $2p_z$ orbital of central carbon. These types of clusters stabilized by the electronic approach, as proposed by Hoffmann and co-workers, have similar σ - and/or π -delocalized MOs, which are responsible for the stability of the clusters in planar forms. For the neutralization of these mono-anionic clusters, Li^+ ions are used and the systems are denoted as Li@SiGaAl_2 and Li@GeGaAl_2 (Figure 6h and 6i, respectively) in which the most favorable site for the bridging of Li^+ ion is to the Al–Al bonds [79]. Interestingly, the Li^+ ion binding on the anionic clusters does not distort the planar geometries. The Li@SiGaAl_2 and Li@GeGaAl_2 clusters also show σ/π -dual aromaticity.

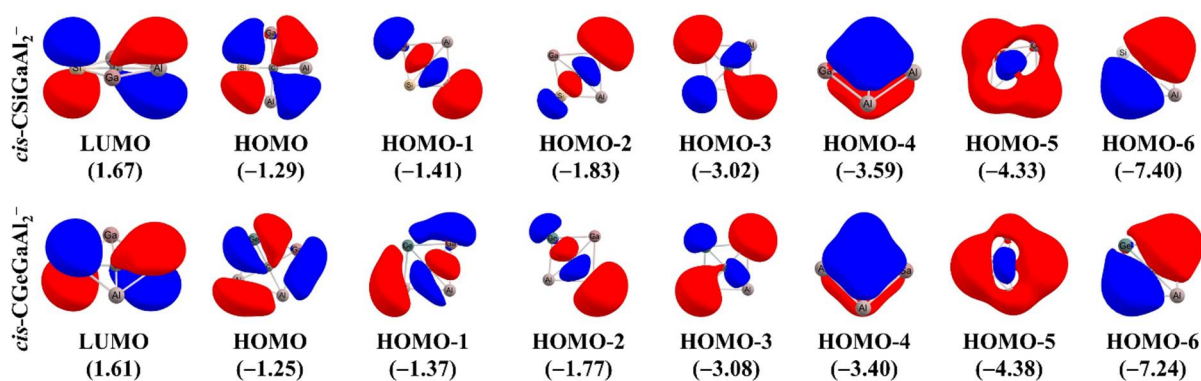


Figure 7. Plots of the molecular orbitals of the global minimum structures of CSiGaAl_2^- and CGeGaAl_2^- clusters. The values in the parentheses are the energies of the corresponding orbitals in the eV unit at the PBE0-D3/def2-TZVPP method.

Using group 14 elements (Si and Ge) as the σ -donating and π -accepting ligand atoms, we have reported ptC global minimum structures in the $\text{CSi}_n\text{Ge}_{4-n}^{2+}$ ($n = 1-3$) clusters (Figure 8a to 8c, respectively) [80]. The exploration of the potential energy surface (PES) with the help of the ABCcluster code [81,82] based on the artificial bee colony algorithm

(ABC) shows that the C_{2v} , D_{2h} , and C_{2v} symmetric ptC structures are the lowest-energy isomers for $CSiGe_3^{2+}$, $CSi_2Ge_2^{2+}$, and CSi_3Ge^{2+} clusters, respectively. This algorithm is a swarm-based intelligence method that was put forth by Karaboga et al. in 2005 [83,84]. It is influenced by the foraging behavior of a bee colony, and only three parameters are required to deal with it. These three parameters are (i) employed honeybees, (ii) onlooker bees, and (iii) food sources. In this algorithm, a colony of artificial forager bees (agents) finds rich artificial food sources (good solutions for a given problem). The studied optimization problem is first transformed into the problem of searching for the best parameter vector that minimizes an objective function. Then, the artificial bees arbitrarily find a population of initial solution vectors and iteratively move towards better solutions while discarding the bad solutions. For the $CSi_2Ge_2^{2+}$ cluster, the second stable structure also has a ptC with $0.67 \text{ kcal mol}^{-1}$ higher energy than the lowest energy ptC isomer. The third stable isomer of $CSi_2Ge_2^{2+}$ and the second stable isomers of $CSiGe_3^{2+}$ and CSi_3Ge^{2+} clusters have more than 10 kcal mol^{-1} higher energy with respect to the lowest-energy ptC structure [80]. All the ptC structures have good kinetic stability against isomerization and decomposition at 300 K and 500 K and 50 ps durations. The systems are σ/π -dual aromatic. The simultaneous σ -donation from the surrounding atoms to the carbon atom and the π -acceptance of the peripheral atoms from the central carbon is predicted from the natural charge analysis [80]. The AdNDP analysis shows the $2\pi/6\sigma$ framework of the ptC core in all the clusters.

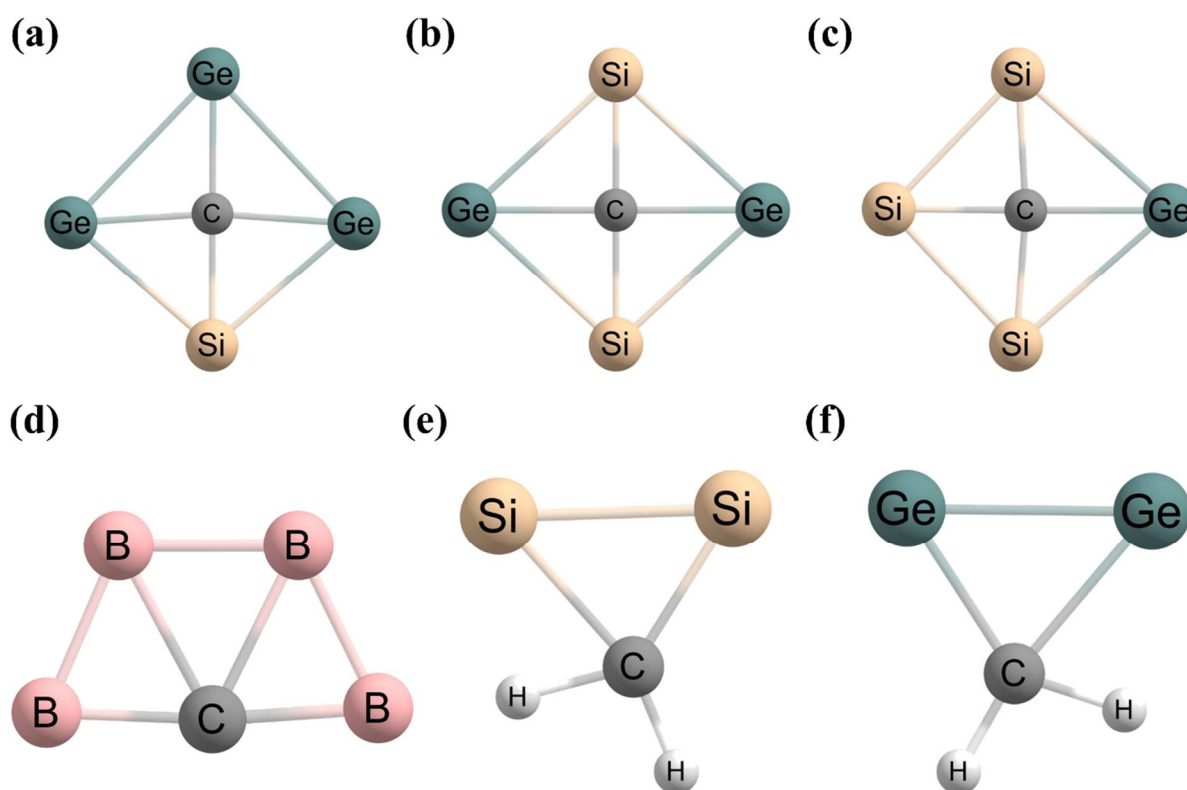


Figure 8. The global minimum structures of (a) $CSiGe_3^{2+}$, (b) $CSi_2Ge_2^{2+}$, (c) CSi_3Ge^{2+} , and (d) CB_4^+ clusters containing a ptC. The local minimum structures of (e) Si_2CH_2 and (f) Ge_2CH_2 molecules.

2.4. Examples of ptCs without 18 Valence Electrons

We have mentioned previously that the totaling of the 18-valence electrons is not a necessary criterion for molecules/ions to show ptCs. This rule can guide the design of new ptC clusters theoretically as well as experimentally. Hence, various neutral and/or ionic clusters were reported to have a ptC without following this criterion, and the clusters show stability in the planar forms. The global minimum geometry of a 15-valence electronic mono-cationic CB_4^+ system contains a ptC, which was reported by Merino and co-workers

in 2011 (Figure 8d) [85]. They found a planar tetracoordinate boron (ptB) center in the global minimum structure of the CB_4 system, which agrees with the results of Boldyrev and Wang. The lowest-energy ptC isomer is in the doublet state for the CB_4^+ system and is more stable by 30 kcal mol^{-1} energy than the quartet states of the cluster. The interesting fact is that Becker and Dietze observed this cluster via laser mass spectrometry of boron carbide in 1988 and the ground state has a ptC structure [86].

Vogt-Geisse et al. in 2015 announced a local minimum geometry of two 14-valence electronic Si_2CH_2 and Ge_2CH_2 species with a ptC (Figure 8e and 8f, respectively) [87]. The ptC isomers have 25.1 and $17.2 \text{ kcal mol}^{-1}$ higher energy with respect to the lowest-energy isomer for Si_2CH_2 and Ge_2CH_2 systems, respectively. From the natural bond orbital (NBO) analysis, they proposed the presence of an out-of-plane 3c–2e Si–C–Si and Ge–C–Ge π -bond generated by the delocalization of the lone pair on the central carbon into the empty *p*-orbitals of silicon and germanium atoms [87]. Additionally, hydrogen-bridged 3c–2e Si–H–C and Ge–H–C bonds exist in the ptC isomers of the Si_2CH_2 and Ge_2CH_2 systems, respectively.

Another interesting work by the group of Hou, Gu, and Li reported the 12-valence electronic ptC species CLi_3E ($\text{E} = \text{N}, \text{P}, \text{As}, \text{Sb}, \text{Bi}$) and CLi_3E^+ ($\text{E} = \text{O}, \text{S}, \text{Se}, \text{Te}, \text{Po}$) (Figure 9) [88]. The PES search shows the C_{2v} geometries with a ptC are the lowest-energy and most stable in these clusters except for $\text{E} = \text{N}$ and P . In the global minimum ptC structures, a double bond exists among the carbon and E atoms but the C=E bonds in the CLi_3E cluster are unlike those in the CLi_3E^+ cluster. In the global minimum structure of the CLi_3E cluster, the π -electron density disperses between C and E, while for the CLi_3E^+ cluster, it primarily disperses on the E atom. The large energy gap between HOMO and LUMO indicates the stability of both types of complexes in planar orientations [89,90]. Moreover, the CLi_3E^+ type of complexes has a higher energy gap indicating higher thermodynamic stability than the other types of complexes.

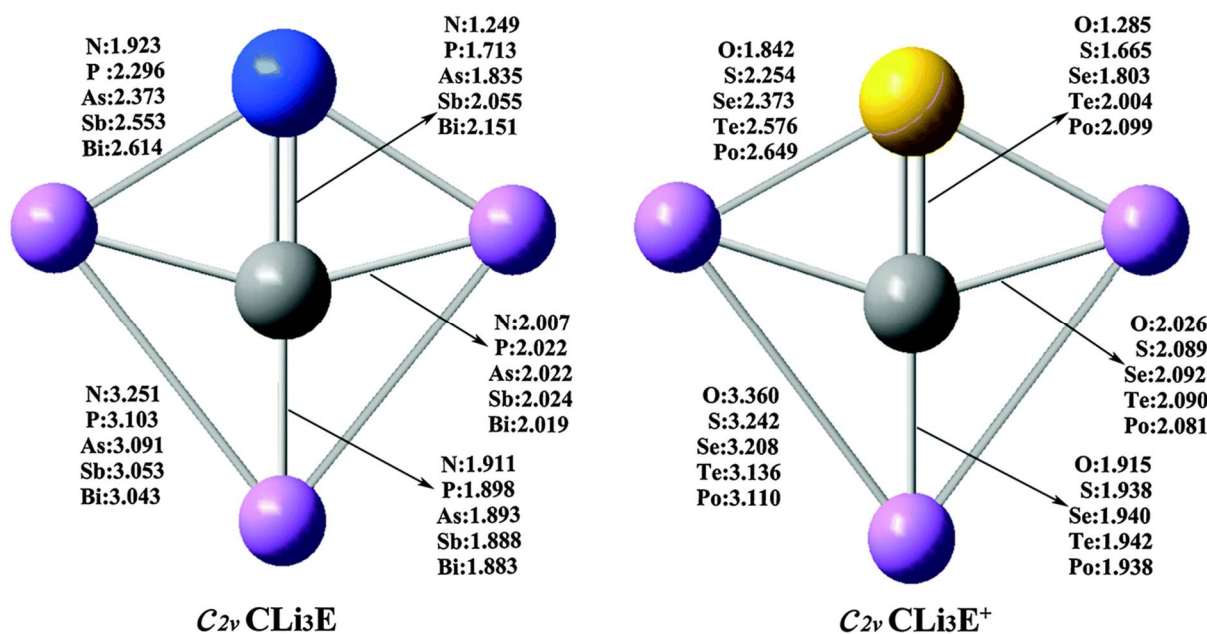


Figure 9. The optimized geometries of $\text{C}_{2v} \text{CLi}_3\text{E}$ ($\text{E} = \text{N}, \text{P}, \text{As}, \text{Sb}, \text{Bi}$) and CLi_3E^+ ($\text{E} = \text{O}, \text{S}, \text{Se}, \text{Te}, \text{Po}$) at the MP2/aug-cc-pVTZ level. Bond distances are in Å. Reprinted from ref. [88] with permission from Royal Society of Chemistry.

In 2018, Zheng et al. designed CAL_3X ($\text{X} = \text{Al}/\text{Ga}/\text{In}/\text{Tl}$) neutral clusters with 16-valence electrons [91]. The exploration of the PES indicated that for CAL_4 (Figure 10a) and CAL_3Ga (Figure 10b) clusters, the global minimum geometries are tetrahedral with 8.70 and $3.66 \text{ kcal mol}^{-1}$ lower energy than the corresponding ptC isomers, respectively.

For the CAI_3In cluster (Figure 10c), the tetrahedral isomer is slightly more stable than the ptC isomer by only $0.69 \text{ kcal mol}^{-1}$. Favorably, for the CAI_3Tl cluster (Figure 10d), the ptC global minimum has $1.01 \text{ kcal mol}^{-1}$ lower energy than the tetrahedral isomer. Hence, only for the CAI_3Tl system, the global minimum structure corresponds to the ptC isomer. Moreover, this ptC isomer has 20 kcal mol^{-1} lower energy than the lowest-energy triplet isomers [91]. Despite the 16-valence electronic cluster, it still shows π -aromaticity. The authors suggested that the ionic $[\text{CAI}_3]^- \text{X}^+$ plays a major role in the competition between tetrahedral and planar isomers of the clusters.

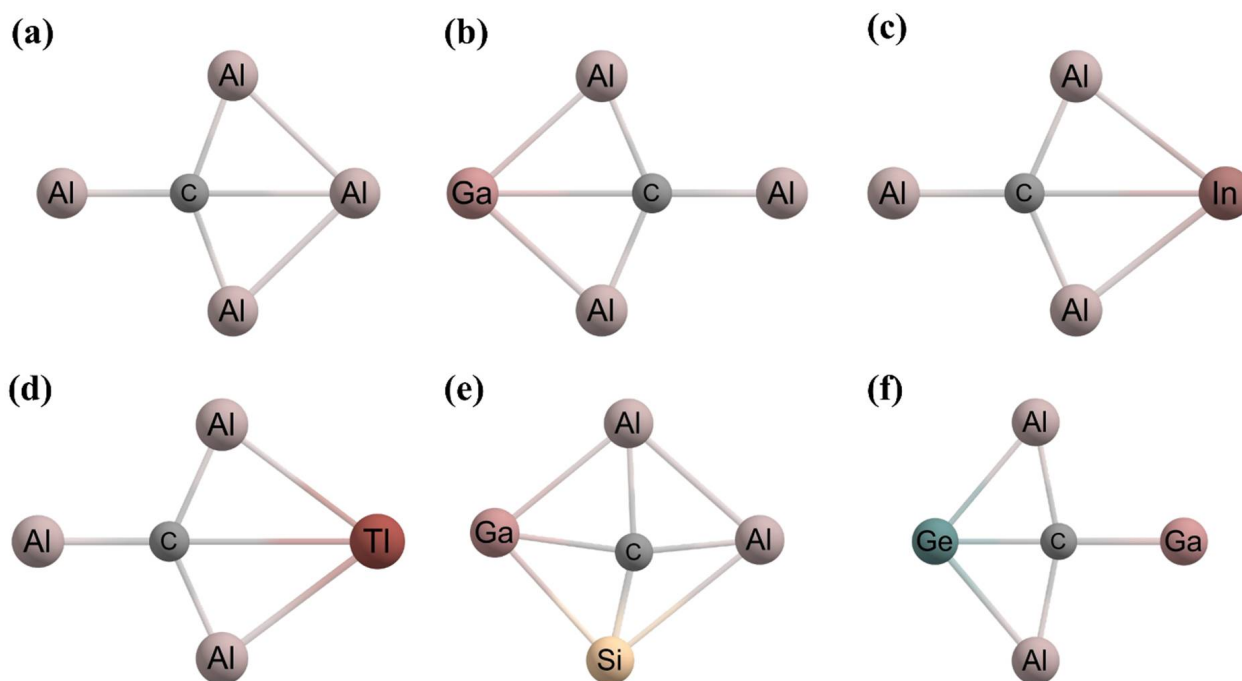


Figure 10. The local minimum structures of (a) CAI_4 , (b) CAI_3Ga , and (c) CAI_3In clusters. The global minimum structure of (d) CAI_3Tl , (e) CSiGaAl_2 , and (f) CGeGaAl_2 clusters with ptCs.

Neutral 17-valence electronic CSiGaAl_2 and CGeGaAl_2 clusters were reported by us (Figure 10e and 10f, respectively) [79]. The PES shows that the lowest-energy structures contain a ptC. The kinetic stability of the clusters was verified at 300 K and 500 K temperatures. The NBO analysis confirmed the σ -electron donation from the surrounding atoms to the carbon center and simultaneously π -back donation occurs from the ptC atom to the ligand atoms. The NICS computations predicted the σ/π -dual aromatic nature of the clusters [79].

Merino and co-workers reported in 2018 the presence of a ptC in the 20-valence electronic CE_5^- ($\text{E}=\text{Al-Tl}$) clusters (Figure 11) [92]. The PES search shows that CAI_5^- and CGa_5^- clusters have a ptC in the global minimum structure with C_{2v} symmetry, whereas CIn_5^- and CTl_5^- clusters have C_{4v} symmetric 3D structures as the global minima with a pentacoordinate carbon atom. Through the systematic bonding analyses, the authors concluded that the ptC clusters (CAI_5^- and CGa_5^-) can be better represented as the CE_4^- fragment collaborates with the E atom. The ptC global minimum structures have both σ and π dual aromaticity with the σ term as the governing term.

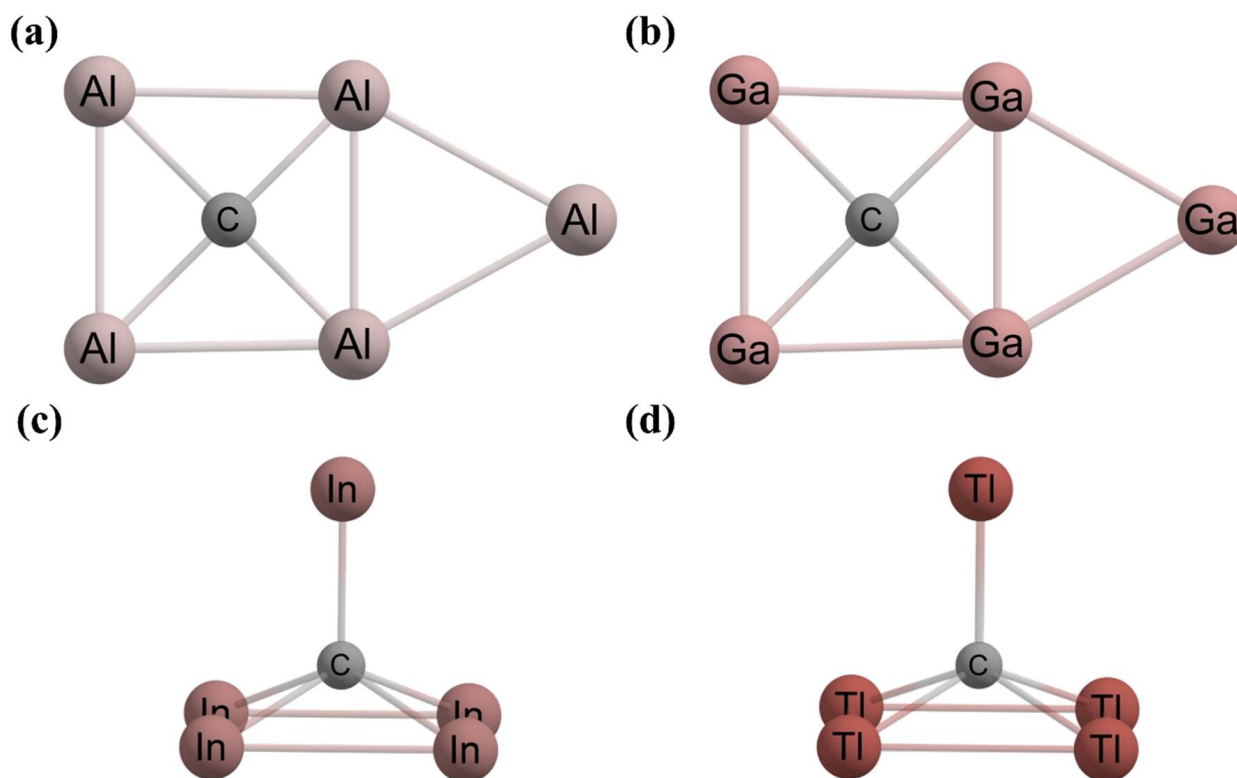


Figure 11. The global minimum structures of (a) CA_{15}^- , (b) CGa_5^- , (c) CIn_5^- , and (d) CTl_5^- clusters.

Another 12-valence electronic system, $CBe_3X_3^+$ ($X = H, Li, Na, Cu, Ag$) (Figure 12), was predicted by Guo et al. in 2019 [93]. The PES search shows that the ptC structures are global minima, in which the central carbon is connected to three in-plane beryllium (Be) atoms and a terminal X center. The remaining two X atoms are present at the perimeter and each bridge with two beryllium atoms. The second most stable geometries for $CBe_3X_3^+$ ($X = H, Li, Na, Cu, Ag$) have 3.66, 3.98, 1.90, 7.91, and 5.92 kcal mol⁻¹ higher energies as compared to the corresponding lowest energy ptC isomers, respectively [93]. The bonding analyses predicted that the eight electrons are used for delocalized $2\pi/6\sigma$ bonding on the ptC moiety and the remaining four electrons are used for the surrounding Be–X–Be and Be–Be σ -bonding. The global minimum ptC isomers have π/σ dual aromaticity. The molecular dynamics simulations at 300 K for 50 ps suggest that the ptC structures are kinetically stable enough against isomerization and decomposition.

Furthermore, Wu et al. recently designed 14- and 16-valence electronic CLi_2AlE and $CLiAl_2E$ ($E = P, As, Sb, Bi$) clusters (Figure 13), respectively [94]. The PES exploration indicated the global minimum structures have a ptC except for the $CLiAl_2P$ cluster. In these species, the formation of the C=E bonds is crucial to stabilizing the clusters in planar orientations. The systematic bonding analyses of the clusters show the appearance of three σ and one π bonds among the carbon and surrounding ligand atoms. The ptC geometries have good kinetic stability at 298 K temperature. The NICS computations predicted the σ/π -dual aromaticity of the ptC structures, which are in support of the stability of the clusters.

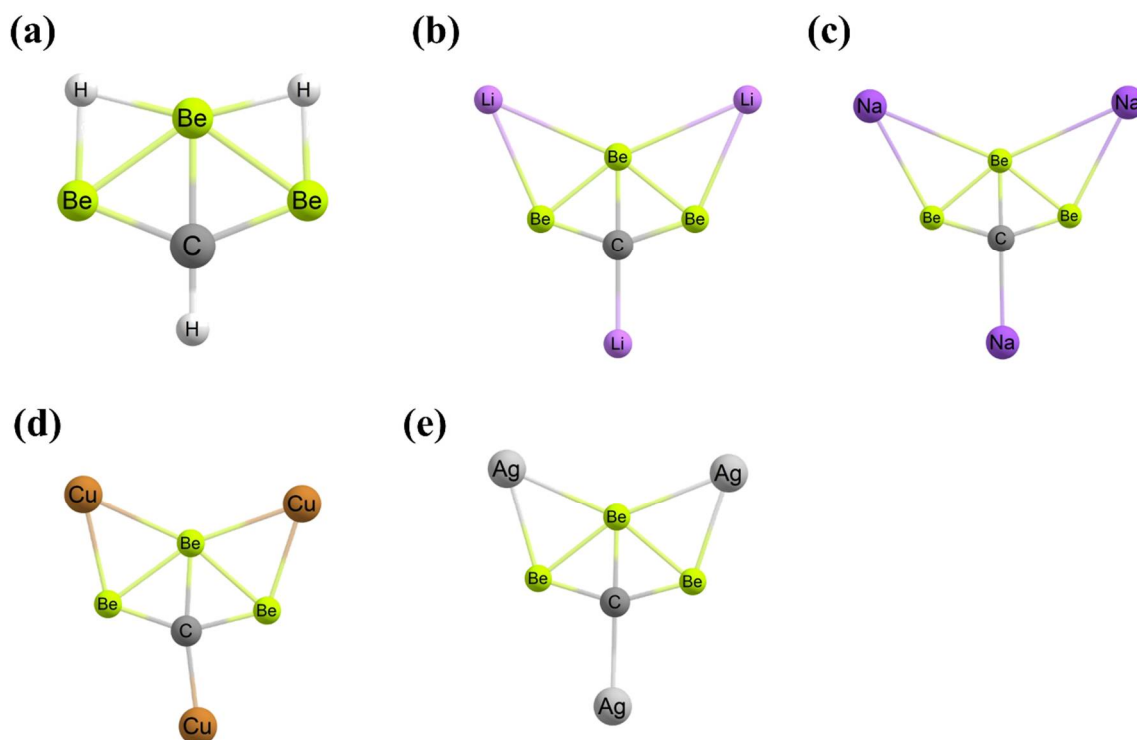


Figure 12. The global minimum structures of (a) CBe_3H_3^+ , (b) $\text{CBe}_3\text{Li}_3^+$, (c) $\text{CBe}_3\text{Na}_3^+$, (d) $\text{CBe}_3\text{Cu}_3^+$, and (e) $\text{CBe}_3\text{Ag}_3^+$ clusters.

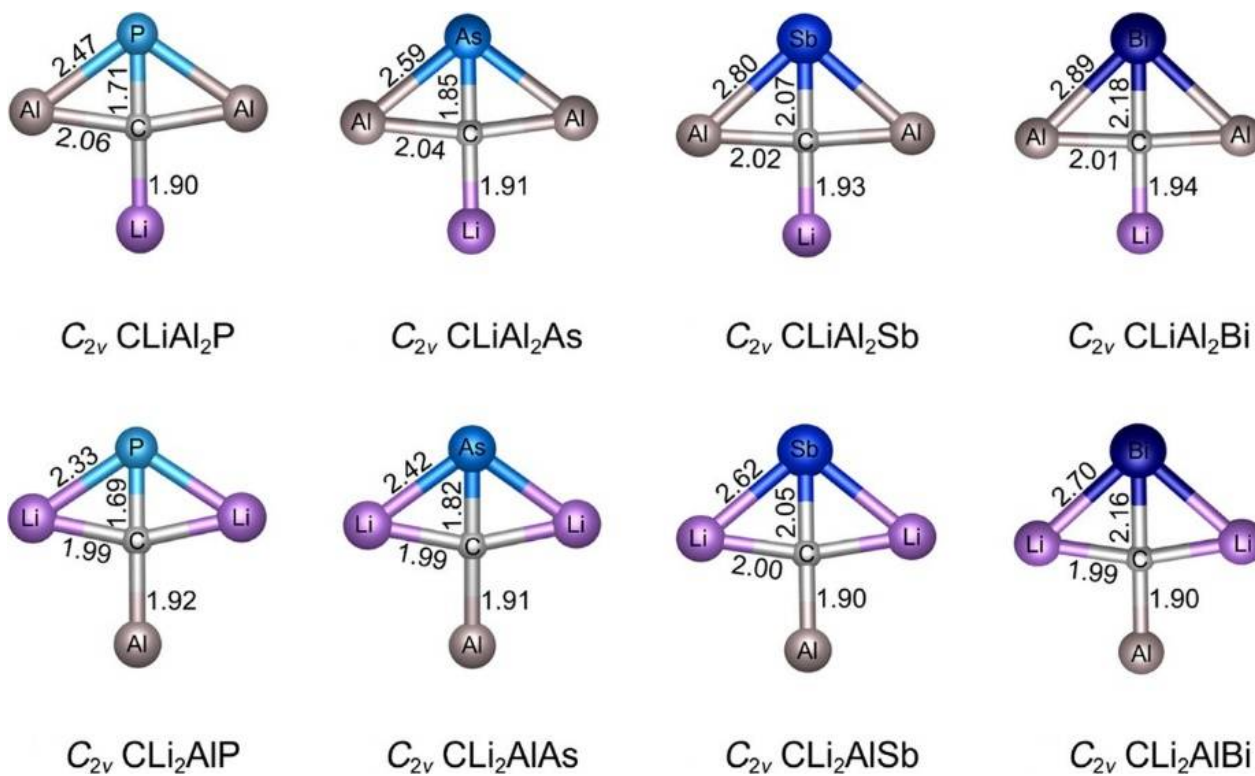


Figure 13. Optimized ptC global minimum structures of $\text{C}_{2v} \text{CLiAl}_2\text{E}$ and CLi_2AlE ($\text{E} = \text{P, As, Sb, Bi}$) at B3LYP/C, Li, Al, P, As/aug-cc-pVTZ/Sb, Bi/aug-cc-pVTZ-pp levels. Bond distances are in Å.

In 2021, Job et al. designed a 19-valence electronic CAI_4Mg^- system (Figure 6b) with a ptC atom in the global minimum energy structure [66]. The second-lowest isomer has

10.13 kcal mol⁻¹ higher energy than the ptC isomer. The ptC structure exhibits σ/π double aromaticity as confirmed by the NICS calculations. The natural charge analysis shows that the central carbon behaves as simultaneous σ -acceptor and π -donor.

In 2021, Leyva-Parra et al. designed and explored the PES of $M_mCE_2^p$ (E=S–Te, M=Li–Cs, $m=2, 3$ and $p=m-2$) and $M_nCE_3^q$ (E=S–Te, M=Li–Cs, $n=1, 2$ and $q=n-2$) systems (Figure 14) [95]. They found that among 38 global minima, 24 are ptCs and 14 are ppCs species. All of the ptCs and ppCs that have been recognized as potential global minima with C_{2v} (M_2CE_3 , MCE_3^- , and $M_3CE_2^+$) or C_s (M_2CE_2) geometries have C–E bond lengths between single and double bonds. In all of these systems, covalent connections between carbon and chalcogens and favorable electrostatic attractions between carbon and alkali metals are confirmed by chemical bonding analyses. Thus, all of these systems satisfy the geometric and electronic requirements for classification as systems with planar hypercoordinate carbon atoms. Furthermore, the detected systems are dynamically stable, suggesting that their experimental validation at room temperature is feasible.

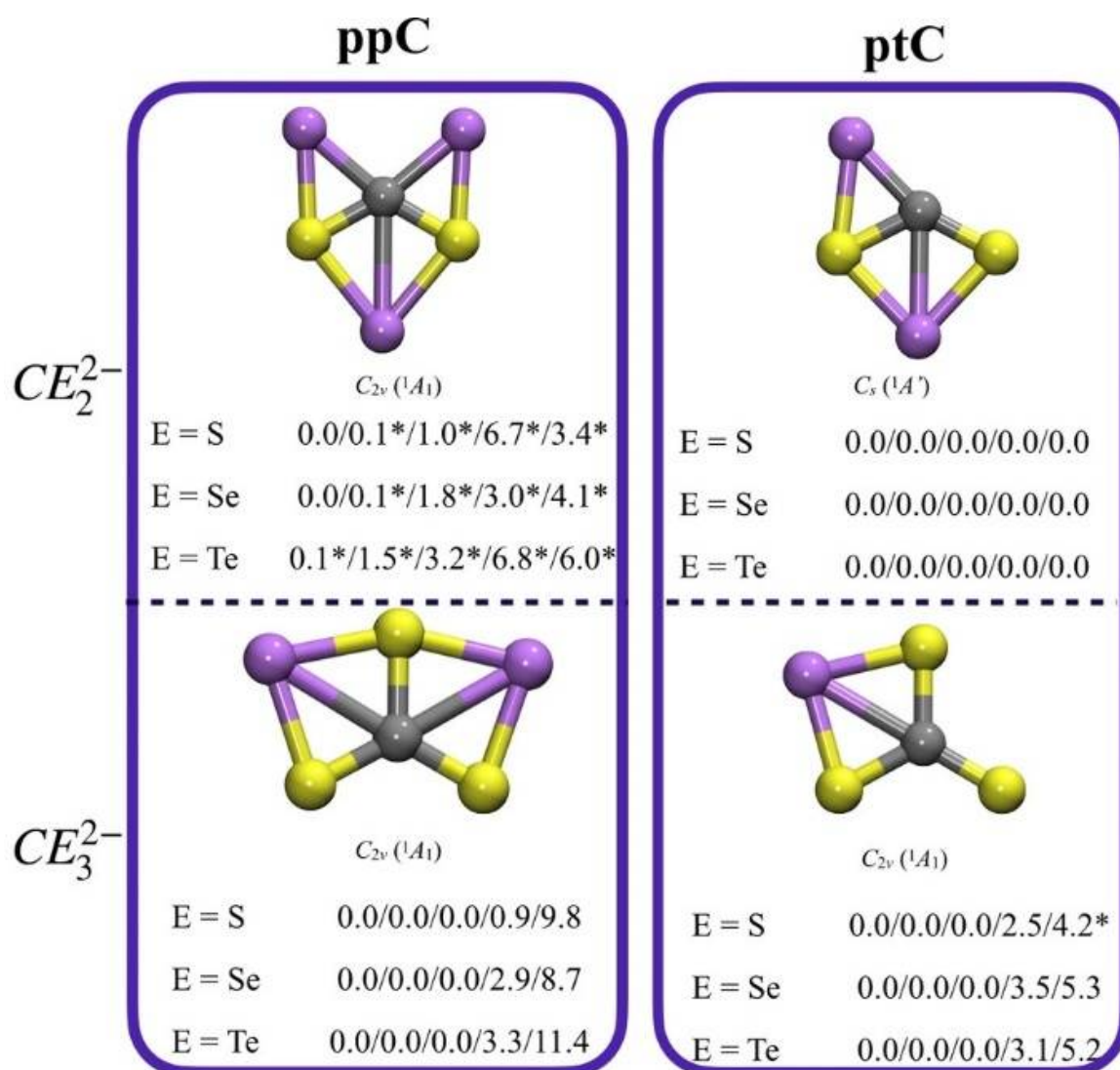


Figure 14. The ppC- and ptC-optimized structures resulting from the alkali metal decoration of CE_3^{2-} and CE_2^{2-} dianions ($M_3CE_2^+$, M_2CE_2 , M_2CE_3 , and MCE_3^-). Point group symmetries, electronic states, and relative energies (kcal mol⁻¹) at the CCSD(T)/def2-TZVP//PBE0-D3/def2-TZVP level. The relative energies follow the Li/Na/K/Rb/Cs order. (Reprinted from ref. [95] with permission from Wiley. Copyright © 2022 Wiley-VCH GmbH).

2.5. Examples of ptCs Using New Principles

In 2017, Merino and co-workers proposed stable ptC-containing compounds embedded in aromatic hydrocarbons [96]. They used such types of ligands that have empty orbitals and do not change the sp^2 hybridization of the aromatic carbons. With the use of the empty orbitals that are perpendicular to the aromatic rings, the ligands take part in the aromatic π -electronic delocalization. Under these two situations, the ligands encourage the formation of a three-centered-two-electron σ -bond with the ptC atom. The authors found a ptC global minimum for the $Si_2C_5H_2$ cluster (Figure 15a) for which the next lowest-energy isomer has $24.6 \text{ kcal mol}^{-1}$ higher energy than the ptC isomer. Moreover, $Ge_2C_5H_2$, $Ge_2C_6H_3^+$, $Sn_2C_5H_2$, $Sn_2C_6H_3^+$, $Pb_2C_5H_2$, $Pb_2C_6H_3^+$, and $Si_2C_6H_3^+$ clusters also have a ptC in the global minimum structures (Figure 15) [96].

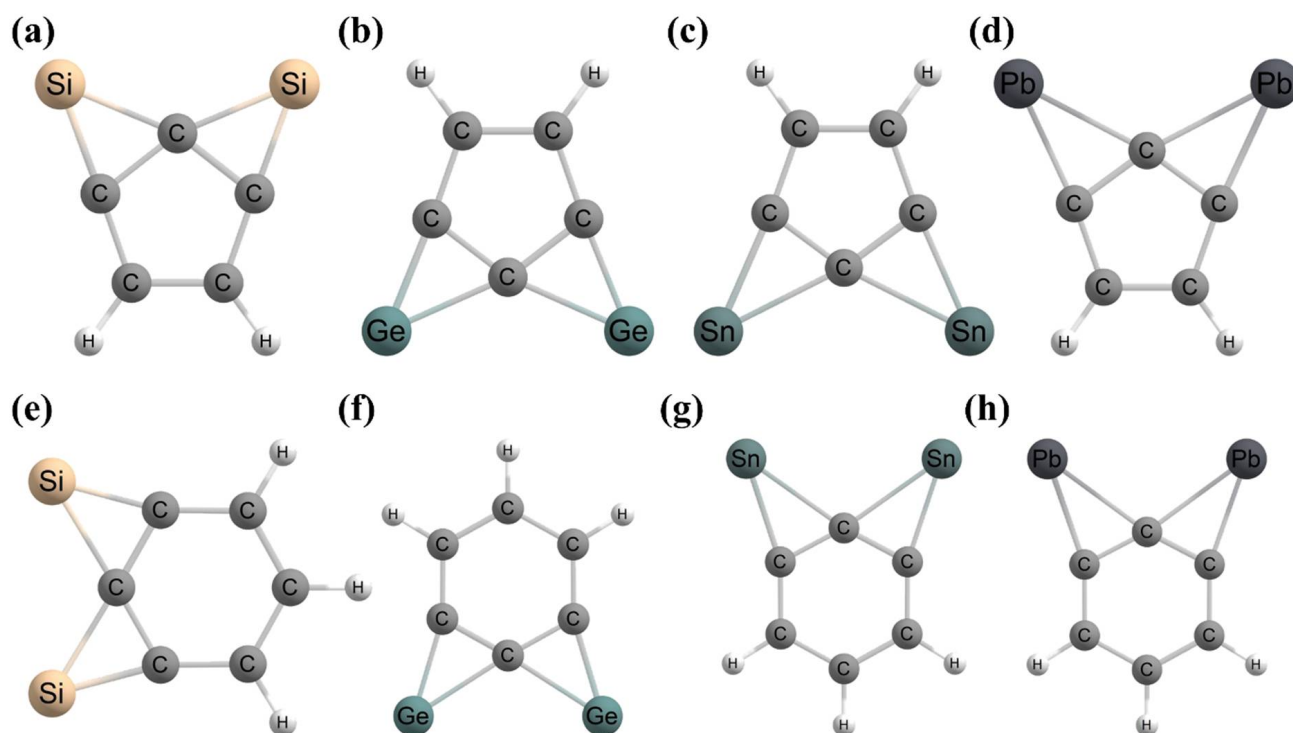


Figure 15. The optimized structures of cyclic aromatic hydrocarbons (a) $Si_2C_5H_2$, (b) $Ge_2C_5H_2$, (c) $Sn_2C_5H_2$, (d) $Pb_2C_5H_2$, (e) $Si_2C_6H_3^+$, (f) $Ge_2C_6H_3^+$, (g) $Sn_2C_6H_3^+$, and (h) $Pb_2C_6H_3^+$ clusters.

The presence of the ptC center in the allene-type structures was reported by the group of Merino and co-workers in 2021. They explored the PES of the CE_2M_2 ($E = Si-Pb$; $M = Li$ and Na) clusters (Figure 16a) [97]. In the case of CE_2Li_2 clusters, the global minima and also the second lowest structures have a ptC. However, for the CE_2Na_2 , except for CPb_2Na_2 , all other clusters have a ptC in the global minimum geometries with D_{2h} symmetry. For the CPb_2Na_2 cluster, the ptC geometry has $1.0 \text{ kcal mol}^{-1}$ higher energy than the most stable tricoordinate carbon structure. The design, based on a π -localization strategy, appeared in a ptC with two double bonds to establish a linear or bent allene-type $E=C=E$ fragment. The magnetic response study shows the σ -delocalization by the bent allene-type $E=C=E$ moiety, which has a crucial role in maintaining the stability of the clusters. Through the bonding analyses, the authors concluded the ionic nature of the C–M bonds and the covalent nature of the C–E bonds.

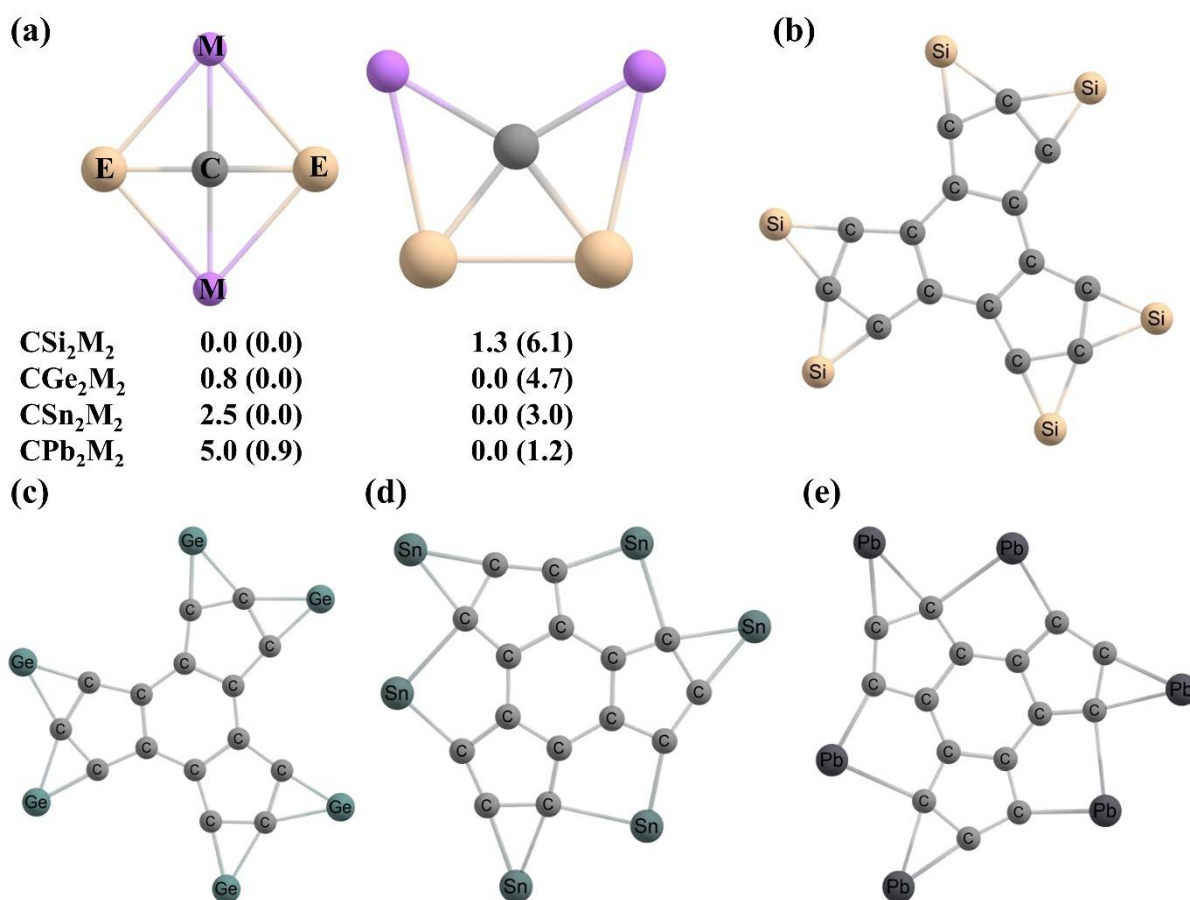


Figure 16. (a) The structure and relative energies (kcal mol^{-1}) of the global minima and second stable isomers of CE_2M_2 ($\text{E} = \text{Si-Pb}$, $\text{M} = \text{Li}$, and Na) at the CCSD(T)/def2-TZVP level. The values without and within parentheses correspond to clusters with Li and Na, respectively. The lowest energy structures of (b) Si_6C_{15} , (c) Ge_6C_{15} , (d) Sn_6C_{15} , and (e) Pb_6C_{15} systems.

Very recently, Inostroza et al. explored the PES of E_6C_{15} ($\text{E} = \text{Si-Pb}$) polycyclic aromatic compounds and reported the presence of three ptCs in the putative global minimum structures of Si_6C_{15} (Figure 16b) and Ge_6C_{15} (Figure 16c) systems with D_{3h} symmetry [98]. However, in the case of Sn_6C_{15} (Figure 16d) and Pb_6C_{15} systems (Figure 16e), due to the large size of Sn and Pb atoms, the global minimum is a bowl-shaped geometry with three quasi-ptCs. Three ptCs are also present in the second stable isomers of Si_6C_{15} and Ge_6C_{15} systems, which are 8.2 and 2.8 kcal mol^{-1} higher in energy compared to the global minimum geometries, respectively. All four lowest-energy isomers have higher HOMO–LUMO energy gaps between 2.13 and 4.03 eV. The C–C bond lengths are within the range of single and double bonds (1.41–1.47 Å), supporting the delocalized character of the bonding. Three delocalized E–ptC–E three-centered-two-electron ($3c-2e$) σ -bonds and nine delocalized π -bonds are found in the chemical bonding study, supporting an aromatic nature in accordance with Huckel's $4n + 2$ rule. The authors show that without disrupting ptC units, these systems may also be employed as a partner to create supramolecular complexes with coronene or [12] cycloparaphenylene ([12] CPPs).

2.6. Examples of Experimentally Predicted ptC Compounds

Interestingly, 17-valence electronic pentatomic CA_4^- and CA_3E ($\text{E} = \text{Si}$, Ge) systems and 18-valence electronic CA_3E^- ($\text{E} = \text{Si}$, Ge) were detected in a photoelectron spectroscopy experiment and ab initio calculations by Wang as early as 1999 [18,56]. The 16-valence electronic CA_4 molecule has a tetrahedral geometry and the CA_4^- system has a planar geometry with D_{4h} symmetry (Figure 17a). The experimental vertical detachment energy

(VDE) of CAI_4^- is approximately 2.65 ± 0.06 eV, which is in good agreement with the computed value of 2.71 eV. The authors stated that the tetrahedral CAI_4 molecule should have a $1a_1^2 1t_2^6 2a_1^2 2t_2^6 1e^0$ electronic arrangement, which represents four σ bonds ($1a_1$ and $1t_2$) and four lone-pair bonds ($2a_1$ and $2t_2$). Adding one extra electron to the $1e$ LUMO gives the $1a_1^2 1t_2^6 2a_1^2 2t_2^6 1e^1$ electronic arrangement for the CAI_4^- cluster. As the $1e$ orbital is unsymmetrically filled, it is expected to show Jahn–Teller distortion to give a D_{4h} symmetric planar structure (Figure 17a). The planarity in the CAI_4^- cluster is accomplished by the ligand–ligand bonding relationships in the HOMO. For the CAI_3Si system, the authors predicted two planar low-lying C_{2v} -I (Figure 17b) and C_{2v} -II (Figure 17c) structures, but the C_{2v} -I isomer has $2.5 \text{ kcal mol}^{-1}$ lower energy than the C_{2v} -II isomer. Moreover, the C_{2v} -I isomer has $7.8 \text{ kcal mol}^{-1}$ lower energy than the tricoordinate C_s isomer. Hence, they mentioned that in the case of the CAI_3Si cluster, the C_{2v} -I isomer is the global minimum structure [56]. Similar to the CAI_3Si cluster, the CAI_3Ge system has two minima C_{2v} -I (Figure 17b) and C_{2v} -II (Figure 17c) [56]. In the case of the CAI_3Si^- and CAI_3Ge^- systems, the C_{2v} symmetric ptC structures (Figure 17b) were reported as the lowest-energy isomers. In all these clusters, the appearance of a four-center bond was discovered to be crucial for the stability of the ptC isomers.

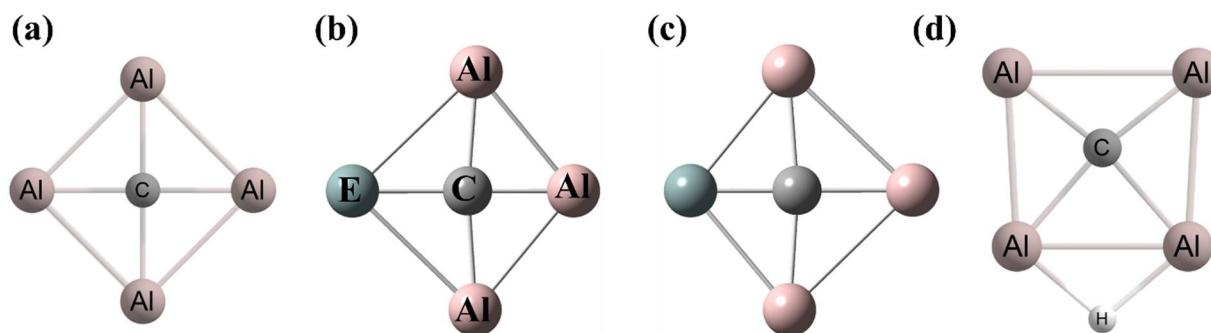


Figure 17. The optimized structures of (a) CAI_4^- , (b) CAI_3E (E = Si, Ge) (C_{2v} -I) and CAI_3E^- , and (c) CAI_3E (E = Si, Ge) (C_{2v} -II) clusters. The global minimum structures of (d) CAI_4H and CAI_4H^- clusters. For (b,d) structures, the neutral and anionic forms have the same shape but different bond lengths.

In 2017, Xu et al. reported a combined experimental and theoretical study of CAI_4H and CAI_4H^- clusters based on anion photoelectron spectroscopic and quantum mechanical methods [99]. The authors showed that the most preferable binding site of H is bridging to the Al–Al bond instead to bind with one Al atom in both these clusters (Figure 17d). The neutral and mono-anionic species have 17- and 18-valence electrons, respectively. For the CAI_4H cluster, the experimental electron affinity (EA) value is 2.6 eV. In the case of the CAI_4H^- cluster, the experimental VDE is 2.88 eV, in good agreement with the computed VDE of 2.75 eV indicating its high stability [99]. The PES search shows the ptC isomers with a bridging H as global minimum structures for both these clusters. The molecular orbital analysis predicts the delocalized π orbitals, which play an important role in maintaining the planar structure of the clusters, and the species show aromatic character. The acceptable agreement between experimental and computational studies concludes that the ground state of $\text{CAI}_4\text{H}^{-/0}$ clusters have ptC.

3. Planar Pentacoordinate Carbons (ppCs)

The idea of ptC is expanded to the probability and representation of systems with ppC centers [100]. In 1995, Bolton et al. reported the singlet 1,1-dilithioethene molecule (Figure 18a) with the help of the ab initio quantum mechanical methods, which show the ppC local minimum structure having $7.2 \text{ kcal mol}^{-1}$ more energy compared to the lowest-energy isomer with a ptC atom [101]. The barrier height for the interconversion between

the ppC and the lowest-energy ptC isomers is approximately $0.4 \text{ kcal mol}^{-1}$ indicating that it is impossible to characterize the ppC isomer experimentally.

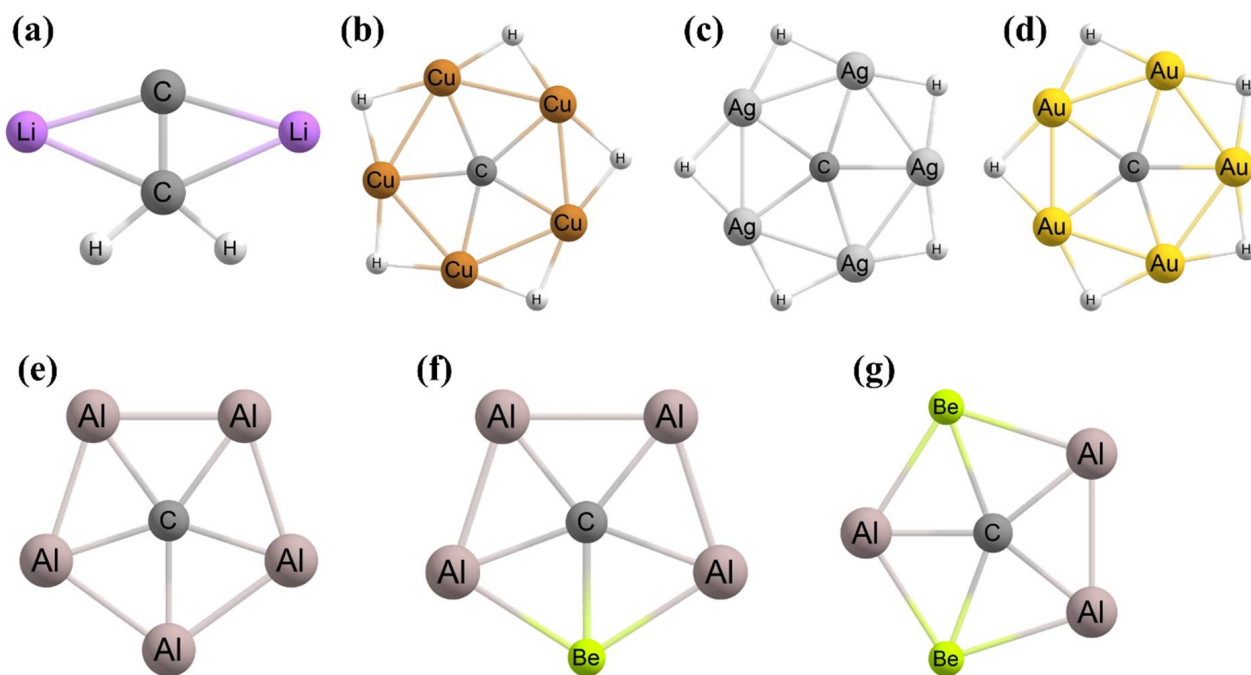


Figure 18. (a) A C_{2v} -symmetric ppC-containing isomer of 1,1-dilithioethene contains two bridging Li centers. The computed structures of (b) $\text{Cu}_5\text{H}_5\text{C}$, (c) $\text{Ag}_5\text{H}_5\text{C}$, and (d) $\text{Au}_5\text{H}_5\text{C}$ each feature bridging hydrides and a ppC. The global minimum energy structures of (e) CA_{15}^+ , (f) CA_{14}Be , and (g) $\text{CA}_{13}\text{Be}_2^-$ clusters.

Wang and Schleyer suggested the design principles of “hyparenes” and reported a family of systems with ppC using density functional theory (DFT)-based computations [102]. They predicted that it is possible to construct “hyparenes” with the replacement of the $-(\text{CH})_3-$ groups in aromatic and/or antiaromatic hydrocarbons by three borocarbon units with ppCs $-\text{C}_3\text{B}_3-$ (Type I), $-\text{C}_2\text{B}_4-$ (Type II), and $-\text{CB}_5-$ (Type III) (Figure 19). The uncommon geometries of the hyparenes can offer unique characteristics that are of use to compose new materials. The hyparenes correspond to the low-lying local minima with normal C–B, B–B, and C–C bond distances. The partial σ and partial π bonds to the planar pentacoordinate carbons contributed to the multicenter bonding in the hyparenes. After the detection of the aromatic $\text{M}_5(\mu\text{-H})_5$ hydrometal rings ($\text{M} = \text{Cu}, \text{Ag}, \text{Au}$) [103,104], Li et al. placed one carbon atom at the center of the $\text{Cu}_5(\mu\text{-H})_5$ ring and found a perfect D_{5h} symmetric true local minimum structure with a ppC (Figure 18b) [105]. Although the $\text{Cu}_5(\mu\text{-H})_5$ ring is aromatic in nature, the inclusion of the carbon causes the nonaromaticity of the ring. Further, the $\text{Ag}_5\text{H}_5\text{C}$ (Figure 18c) and $\text{Au}_5\text{H}_5\text{C}$ (Figure 18d) molecules also have a ppC in their local minimum geometries [106].

The first global minimum geometry with a ppC in the CA_{15}^+ system with D_{5h} symmetry (Figure 18e) was reported based on an extensive PES search in 2008 by Zeng and co-workers [107]. This ppC geometry is $3.8 \text{ kcal mol}^{-1}$ lower in energy than the second-lowest C_{2v} isomer of this system. This system is also consistent with the electronic stabilization strategy approach given by Hoffmann and coworkers, and the presence of the back donation from the central carbon to the peripheral atoms is also reported by them. Moreover, the aromaticity analysis based on the NICS computations of this ppC system has been carried out by these groups.

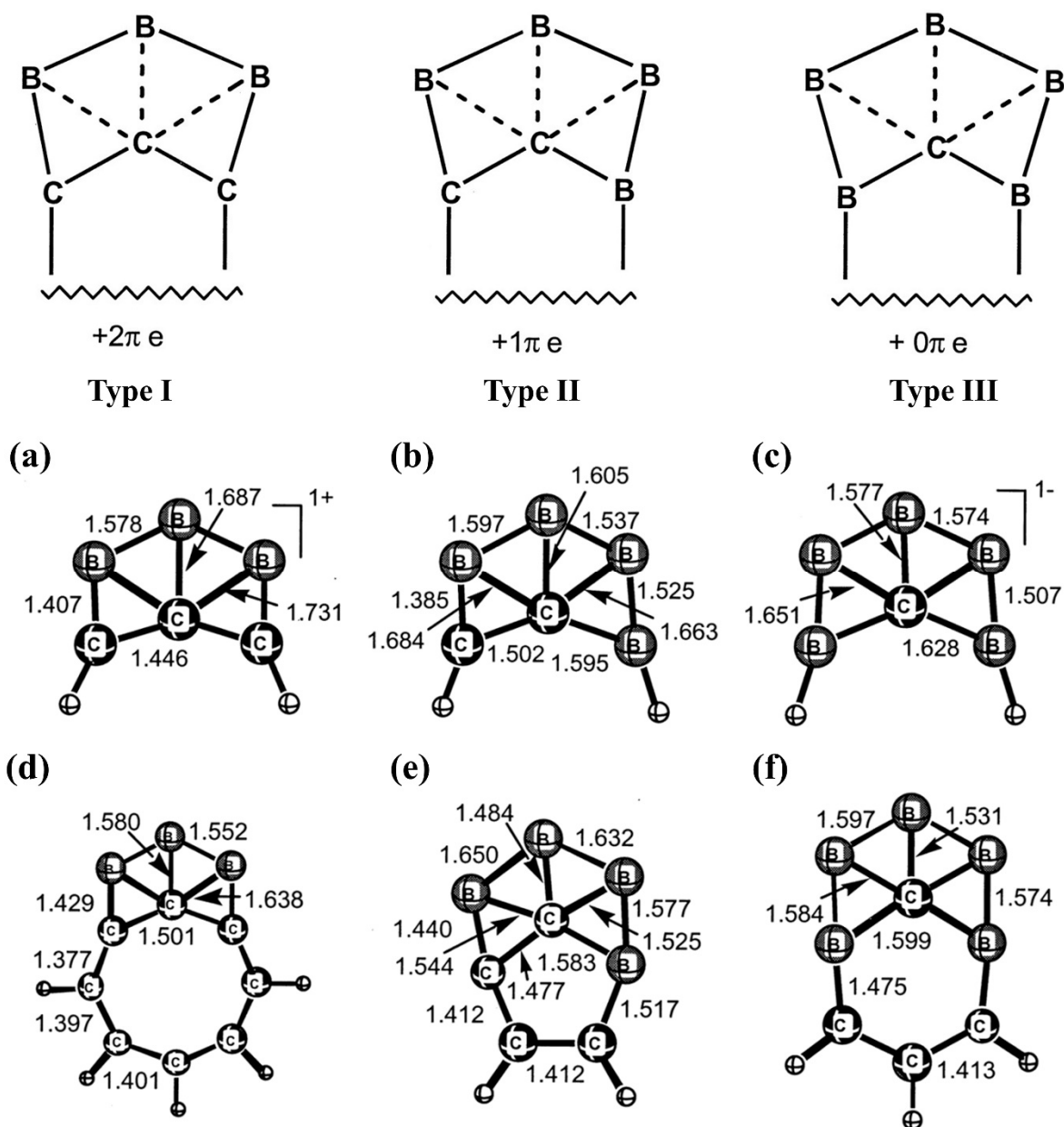


Figure 19. Conceptual relation of the building unit types (I,II,III) to stable isoelectronic 4π species with planar pentacoordinate carbons (a–c) and the hyparenes (d–f). Adapted from ref. [102] with permission from the American Association for the Advancement of Science. Copyright © 2022, The American Association for the Advancement of Science.

After one year, Wang and coworkers substituted the Al atoms with isoelectronic Be atoms to generate neutral CAI_4Be (Figure 18f) and mono-anionic $CAI_3Be_2^-$ (Figure 18g) systems containing ppCs in the global minimum structures [108]. The aluminum–carbon bond distances are between 2.08 and 2.29 Å, which are somewhat lengthy compared to the value of the normal aluminum–carbon bond distance of 2.00 Å but close to the 2.12 Å values as predicted theoretically for the CAI_5^+ system. The bonds among the central carbon and the surrounding Be and Al atoms are longer by 0.08 Å to 0.29 Å than the corresponding normal values. The molecular dynamics simulation suggested the dynamic stability of these global minimum ppC isomers. The highly negative charges on the carbon are the consequences of the σ -donation from the surrounding atoms. At the same time, the carbon lone pair is donated to the ligand atoms. Therefore, the central carbon in the global

minimum structures acts as the σ -acceptor and π -donor. The energy differences between the HOMO and LUMO are 2.6 eV for both ppC structures indicating the greater stability of these isomers [108].

Wu et al., in 2012, reported di-anionic $\text{CAI}_2\text{Be}_3^{2-}$ (Figure 20a) and its mono-anionic salt complex $\text{LiCAI}_2\text{Be}_3^-$ (Figure 20b) systems by further replacement of Al atoms by Be atoms [109]. The PES search shows the global minimum geometry of these clusters has a ppC. The VDE for the $\text{CAI}_2\text{Be}_3^{2-}$ cluster is negative (-1.10 eV) indicating that this species is unstable toward electron release. However, the instability of this cluster is resolved by adding one Li^+ to neutralize one negative charge, and the most preferable binding site of Li^+ is the Be–Be bond in the $\text{LiCAI}_2\text{Be}_3^-$ cluster. In the $\text{LiCAI}_2\text{Be}_3^-$ system, the first computed VDE is 2.28 eV, indicating that the automatic removal of the additional electron is partially eliminated. Moreover, the energy gap between the HOMO and LUMO increases from 0.94 eV in $\text{CAI}_2\text{Be}_3^{2-}$ to 1.79 eV in the $\text{LiCAI}_2\text{Be}_3^-$ system. Hence, from these stability comparisons, it is clear that $\text{LiCAI}_2\text{Be}_3^-$ system is more achievable than the $\text{CAI}_2\text{Be}_3^{2-}$ cluster [109]. The dynamical stability of the global minimum structures was confirmed at 4 K and 298 K temperatures up to 100 ps simulation time. The natural charge analyses indicate that the addition of Li^+ to the $\text{CAI}_2\text{Be}_3^{2-}$ system influences the ionic bonding, but the covalent bonds are not markedly affected.

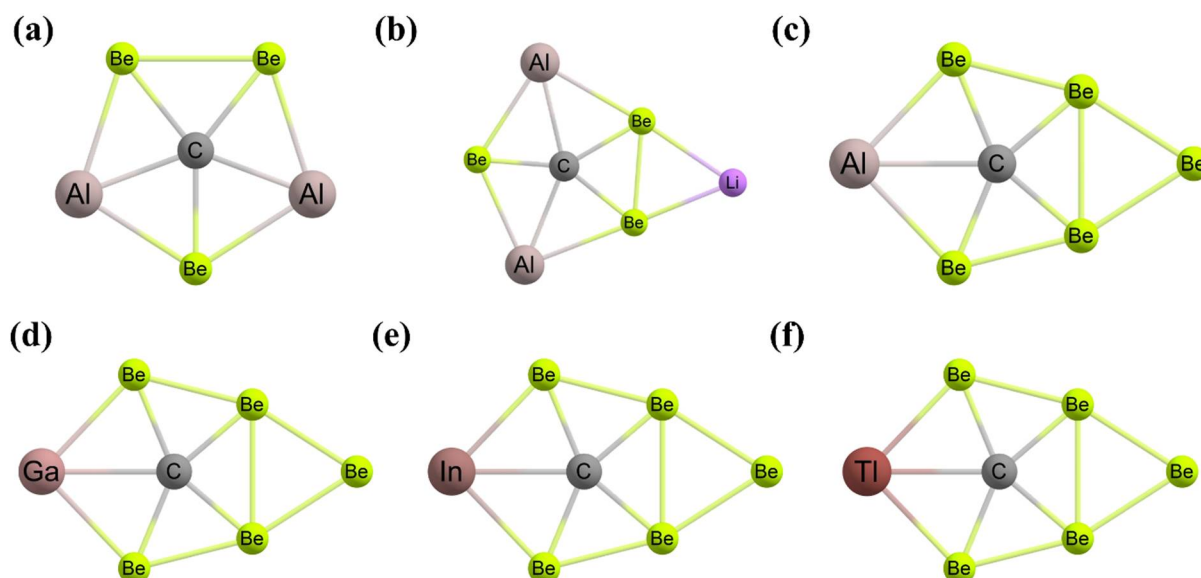


Figure 20. The global minimum energy structures of (a) $\text{CAI}_2\text{Be}_3^{2-}$, (b) $\text{LiCAI}_2\text{Be}_3^-$, (c) CBe_5Al^- , and (d) CBe_5Ga^- clusters. The local minimum structures of (e) CBe_5In^- and (f) CBe_5Tl^- clusters.

Further, the complete substitution of Al atoms was performed by Castro et al., in which they generated heptaatomic anionic clusters CBe_5E^- ($\text{E} = \text{Al}, \text{Ga}, \text{In}, \text{Tl}$) and searched the PES of the designed systems [110]. For CBe_5Al^- (Figure 20c) and CBe_5Ga^- (Figure 20d) clusters, the ppC structures are the global minima. However, for CBe_5In^- (Figure 20e) and CBe_5Tl^- (Figure 20f) clusters, the ppC local minima have only 1.2 kcal mol $^{-1}$ and 1.8 kcal mol $^{-1}$ higher energy compared to the lowest-energy isomers, respectively. The geometries show that the ppC atom is present in the middle of the Be_4E ring, and an extra Be atom is bonded to one Be–Be bond in the plane. In the case of the CBe_5Al^- geometry, the aluminum–carbon bond distance is 2.233 Å, which is somewhat lengthier than the normal aluminum–carbon bond length of 2.00 Å and the 2.12 Å values theoretically predicted for the CAI_5^+ system. The highly negative charges on the carbon are the consequences of the σ -donation from the surrounding atoms. From the valence electronic configuration of the carbon atom, they concluded that the carbon lone pair is donated to the ligand atoms, which assists in stabilizing the planar geometries [110]. The authors found that the planar global minimum geometries are σ - and π -aromatic.

In 2008, Qiong et al. designed CBe_5 and CBe_5^{4-} systems having a ppC atom in their stable local minimum structures (Figure 21a) [111]. The Be_5 ring assists as a σ -donor and a π -acceptor in the D_{5h} structure of CBe_5 and CBe_5^{4-} systems, respectively. The NICS calculations predicted that in the D_{5h} structure of CBe_5 and CBe_5^{4-} systems, σ -aromaticity and π -aromaticity, respectively, are dominant. Although the CBe_5^{4-} cluster has a ppC, the greater charge density makes it unstable. However, the instability of this cluster is resolved by adding Li^+ ions to neutralize the negative charges and the resulting species are $\text{CBe}_5\text{Li}_n^{n-4}$ ($n = 1$ to 5) (Figure 21b to 21f, respectively) [112]. In these clusters, the ppC cores are preserved when Li^+ ions are bonded with their corresponding anions. The central carbon in the global minimum structures acts as the σ -acceptor and π -donor. The electron delocalization within the $\text{CBe}_5\text{Li}_n^{n-4}$ ($n = 1$ to 5) clusters is predicted from the induced magnetic field analysis. The energy gap between the HOMO and LUMO increases moderately upon increasing the counter ions from $\text{CBe}_5\text{Li}_3^-$ (3.47 eV) to $\text{CBe}_5\text{Li}_5^+$ (7.11 eV), suggesting increased stability following the MHP. The molecular dynamics simulations of the systems at 1000 K for 20 ps show that the CBe_5 pentagon remains intact during the entire simulation. The negative charge density on the CBe_5^{4-} cluster is also decreased by capping H^+ ions to the system, just as in the case of Li^+ ions, and the species are $\text{CBe}_5\text{H}_n^{n-4}$ ($n = 2$ –5) [113]. In the case of $\text{CBe}_5\text{H}_2^{2-}$ (Figure 22a) and CBe_5H_3^- (Figure 22b) clusters, the ppC structures are the lowest-energy C_{2v} point group of symmetry. For the CBe_5H_4 cluster (Figure 22c), a quasi-planar geometry has 1.8 kcal mol $^{-1}$ more energy compared to the tetrahedral global minimum structure. Moreover, the CBe_5H_5^+ cluster (Figure 22d) has a quasi-planar ppC structure as the global minimum. The stability of the ppC- or quasi-ppC-containing geometries is governed by the presence of the peripheral three-centered-two-electron Be–H–Be bonds, the origination of the stable eight-electron shell structure, and the presence of the 6σ and 2π dual aromaticity. The excess charge density on the CBe_5^{4-} system is also reduced by complexing with halogen cations (F^+ , Cl^+ , and Br^+) or alkali metal cations (Li^+ , Na^+ , and K^+) to generate CBe_5X_5^+ systems [114]. The PES search shows that the global minima of the clusters are either in ppC or quasi-ppC forms. The global minima of CBe_5F_5^+ , $\text{CBe}_5\text{Li}_5^+$, $\text{CBe}_5\text{Na}_5^+$, and CBe_5K_5^+ clusters (Figure 23) have excellently planar and extremely symmetric D_{5h} geometries, whereas $\text{CBe}_5\text{Cl}_5^+$ and $\text{CBe}_5\text{Br}_5^+$ clusters experience slight non-planar contortion as C_2 geometries (Figure 23). Again, in these systems, the three-centered-two-electron Be–X–Be bonds provide stability in planar forms. The NICS analysis proved the double aromatic character (σ - and π -aromaticity) of the systems is in agreement with the AdNDP analyses. The molecular dynamics simulations suggested that the ppC-containing CBe_5 ring in the minimum energy structures is well conserved throughout the whole simulation, indicating that the geometries are rigid against isomerization and decomposition.

In 2018, Zhao et al. reported various ppC systems by adding hydrogen atoms to the CAI_4Be , $\text{CAI}_3\text{Be}_2^-$, $\text{CAI}_2\text{Be}_3^{2-}$, and CAIBe_4^{3-} parent molecules [115]. They reported nine new planar and quasi-planar ppC clusters of $\text{CAI}_n\text{Be}_m\text{H}_x^q$ ($n + m = 5$, $q = 0, \pm 1$, $x = q + m - 1$) (Figure 24). The ppC core remains unchanged geometrically and electronically with the gradual introduction of hydrogen atoms. Interestingly, the energy gap between the HOMO and LUMO increases in the studied clusters as compared to the parent anionic clusters. The presence of the three-centered-two-electron Be–H–Be or Be–H–Al π bonds is responsible for the stabilization of the ppC geometries [115]. Remarkably, among the nine studied clusters, seven molecules show ppC in the global minimum structures. Again, among the global minimum geometries, only $\text{CAI}_3\text{Be}_2\text{H}$, $\text{CAI}_2\text{Be}_3\text{H}^-$, $\text{CAI}_2\text{Be}_3\text{H}_2$, and $\text{CAIBe}_4\text{H}_4^+$ clusters are dynamically stable enough. For the $\text{CAI}_4\text{BeH}_4^+$ and $\text{CAI}_3\text{Be}_2\text{H}_2^+$ clusters, the ppC isomers have 10.7 and 3.8 kcal mol $^{-1}$ higher energy, respectively, with respect to the lowest-energy structures. However, the closest isomers of the $\text{CAI}_3\text{Be}_2\text{H}$, $\text{CAI}_2\text{Be}_3\text{H}^-$, $\text{CAI}_2\text{Be}_3\text{H}_2$, $\text{CAI}_2\text{Be}_3\text{H}_3^+$, $\text{CAIBe}_4\text{H}_2^-$, CAIBe_4H_3 , and $\text{CAIBe}_4\text{H}_4^+$ clusters have 4.6, 3.1, 4.6, 3.6, 3.7, 2.8, and 15.0 kcal mol $^{-1}$ higher energies, respectively, with respect to the global minimum structures [115]. The NICS calculations predicted that the considered clusters are σ - and

π -dual aromatic. The NBO computations predicted that there is a significant contribution of the ionic and covalent bonding toward the stabilization of the ppC structures.

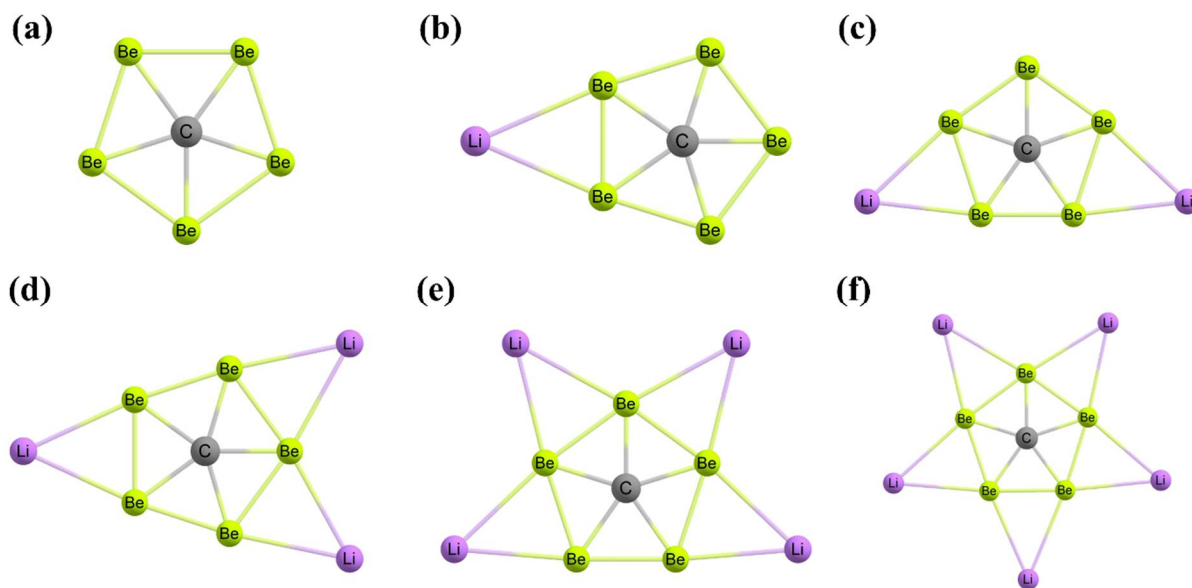


Figure 21. (a) The symmetric structures CBe₅ and CBe₅⁴⁻ are ppC species. The neutral and tetra-anionic forms have the same shape but different bond lengths. The global minimum structures of (b) CBe₅Li₃⁻, (c) CBe₅Li₂²⁻, (d) CBe₅Li₃⁻, (e) CBe₅Li₄, and (f) CBe₅Li₅⁺ clusters.

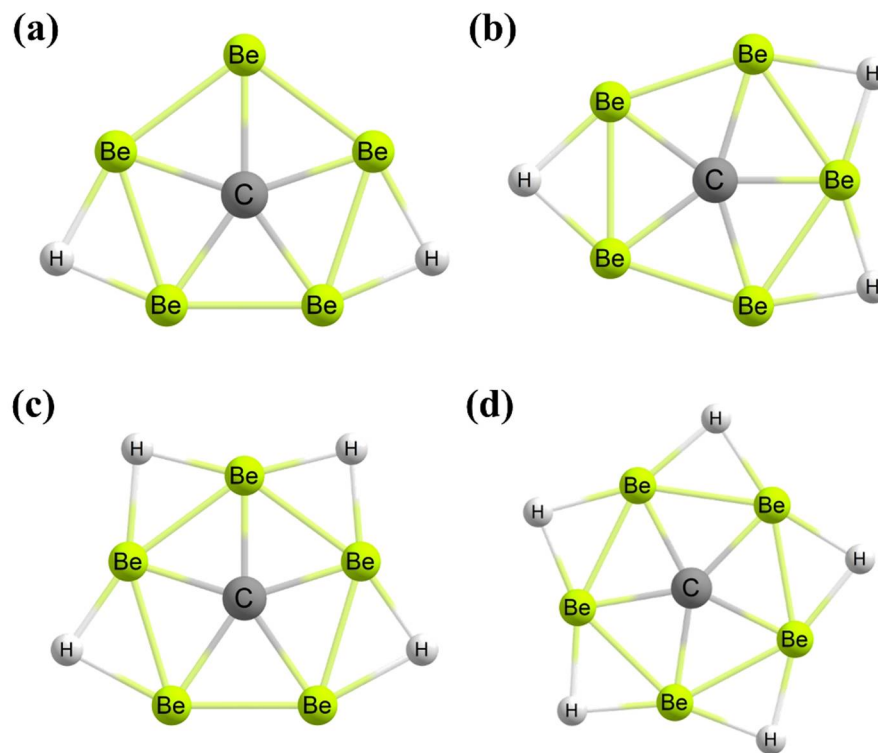


Figure 22. The global minimum structures of (a) CBe₅H₂²⁻ and (b) CBe₅H₃⁻ clusters with a perfect ppC. The local and global minimum structures of (c) CBe₅H₄ and (d) CBe₅H₅⁺ clusters, respectively, with a quasi-ppC.

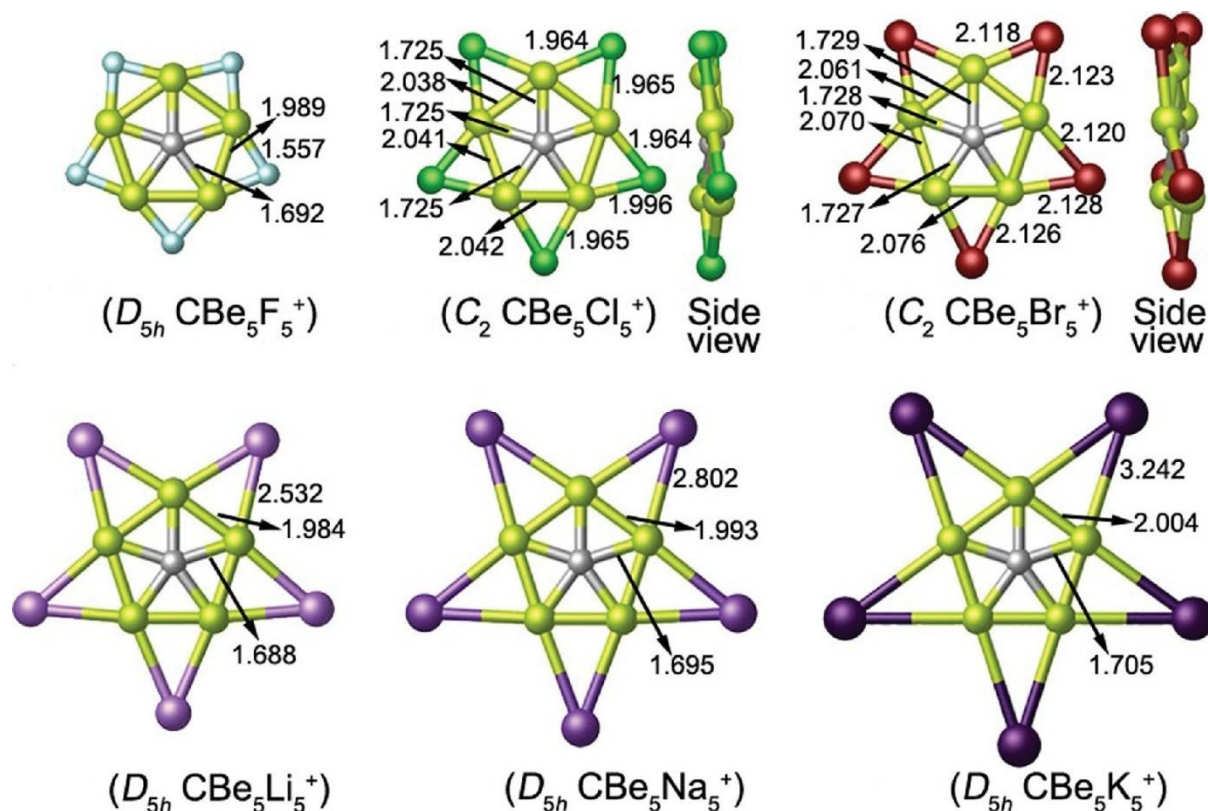


Figure 23. Optimized global-minimum structures of CBe_5X_5^+ ($\text{X} = \text{F}, \text{Cl}, \text{Br}, \text{Li}, \text{Na}, \text{K}$) clusters. Bond distances are indicated in Å. Adapted from ref. [114] with permission from AIP Publishing.

Recently, Pan et al. reported a family of systems with ppC based on the next heaviest analogue of the CAI_5^+ system [116]. As the size of the Ga atom is larger than that of the Al, no ppC isomer is found as a global and/or local minimum for the CGa_5^+ system. Hence, with the use of the smaller-sized beryllium (Be) atoms, the isoelectronic substitution of Ga atoms generated CGa_4Be , $\text{CGa}_3\text{Be}_2^-$, $\text{CGa}_2\text{Be}_3^{2-}$, and CGaBe_4^{3-} clusters with ppC in the global minimum structures (Figure 25). For the neutralization of the anionic clusters, one, two, and three Li^+ ions were used for $\text{CGa}_3\text{Be}_2^-$, $\text{CGa}_2\text{Be}_3^{2-}$, and CGaBe_4^{3-} clusters, respectively, to generate $\text{CGa}_3\text{Be}_2\text{Li}$, $\text{CGa}_2\text{Be}_3\text{Li}_2$, and $\text{CGaBe}_4\text{Li}_3$ clusters (Figure 25). Although the anionic systems have ppC in the global minimum structures, the first ionization potential of $\text{CGa}_2\text{Be}_3^{2-}$ and CGaBe_4^{3-} clusters are negative (-2.91 and -6.45 eV, respectively) suggesting the spontaneous loss of an electron from the clusters [116]. However, the first ionization potential of the $\text{CGa}_3\text{Be}_2^-$ cluster is positive (1.20 eV) indicating its stability towards the spontaneous loss of an electron. The central carbon in the global minimum structures acts as the σ -acceptor and π -donor. Moreover, the extent of π -back-bonding from the $2p_z$ orbital of the central carbon also increases by increasing the number of counter-ions. The electron delocalization within the system is well understood from the molecular orbitals and their magnetic responses studies. The magnetic responses indicated the σ - and π -aromaticity of the global minimum structures, and the σ -contribution is the governing one [116].

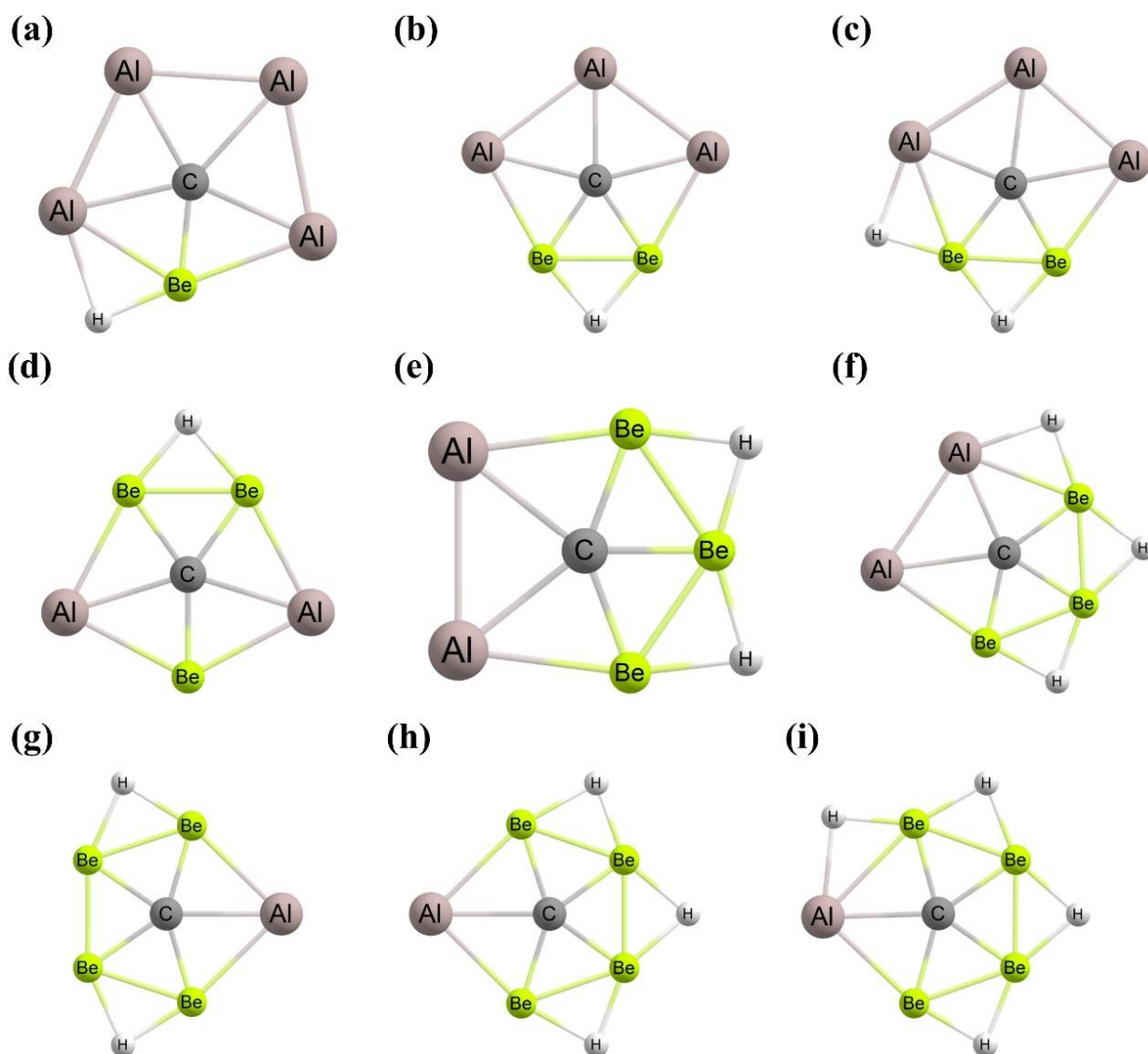


Figure 24. Optimized structures of (a) $CA_{14}BeH_4^+$, (b) $CA_{13}Be_2H$, (c) $CA_{13}Be_2H_2^+$, (d) $CA_{12}Be_3H^-$, (e) $CA_{12}Be_3H_2$, (f) $CA_{12}Be_3H_3^+$, (g) $CA1Be_4H_2^-$, (h) $CA1Be_4H_3$, and (i) $CA1Be_4H_4^+$ clusters.

Using silicon (Si) as the surrounding atoms, Zdetsis et al. in 2011 designed Si_5C^{2-} and Si_5C^- clusters (Figure 26a) with the help of the DFT and the coupled-cluster theory that predicted planar structures of the clusters stabilized by the C–Si bonds [117]. These local minimum structures have 12.9 and 22.8 kcal mol⁻¹ higher energy compared to the three-dimensional-type global minimum for Si_5C^{2-} and Si_5C^- clusters, respectively. For the Si_5C^- cluster, the authors reported two planar structures with D_{5h} and C_s point groups of symmetries that are related by Jahn–Teller distortions. However, these two geometries differ by only 8 kcal mol⁻¹ of energy.

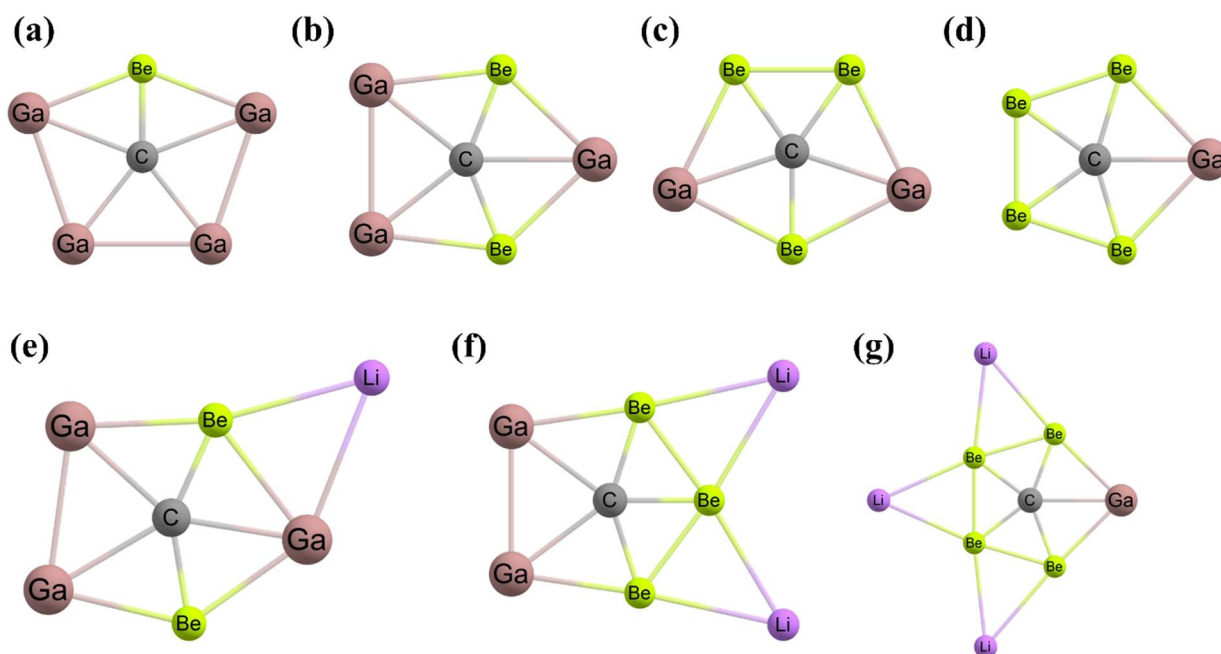


Figure 25. The lowest-energy ppC forms for (a) CGa_4Be , (b) $\text{CGa}_3\text{Be}_2^-$, (c) $\text{CGa}_2\text{Be}_3^{2-}$, (d) CGaBe_4^{3-} , (e) $\text{CGa}_3\text{Be}_2\text{Li}$, (f) $\text{CGa}_2\text{Be}_3\text{Li}_2$, and (g) $\text{CGaBe}_4\text{Li}_3$ clusters.

Merino and co-workers used transition metals along with the main group elements to design a ppC in the global minimum structure. They reported CAI_4MX_2 clusters ($\text{M} = \text{Zr}$ and Hf ; $\text{X} = \text{F-I}$ and C_5H_5) with a ppC connected to a transition metal and attached to a metallocene skeleton (Figure 26b,c) [118]. The natural charge analysis suggested that a significant amount of electron transfer occurs from the surrounding atoms to the central carbon atom and the values are in the range of -2.21 to -2.37 |e|. The BOMD simulations assist the kinetic stability of the Zr systems at 700 K.

Very recently, Sun et al. designed a sulfur-surrounded boron wheel CB_5S_5^+ cluster with a ppC in the global minimum structure (Figure 26d) [119]. In this cluster, the presence of the strong π back-donation from the five-bridged sulfur atoms to the boron atoms lowers the electron-deficient nature of the boron centers. The second-lowest isomer with a ptC atom has $1.1 \text{ kcal mol}^{-1}$ higher energy than the lowest-energy ppC isomer. The structure with planar pentacoordinate boron (ppB) has $61.2 \text{ kcal mol}^{-1}$ higher energy than the ppC structure. The BOMD simulation suggested that at 4 K, the global minimum is dynamically very rigid. Moreover, the planarity of the cluster is well conserved at 298 K, 500 K, and 1000 K temperatures. The considered cluster has a 7.47 eV energy gap between HOMO and LUMO, a high VDE value of 13.22 eV, and a low vertical electron affinity (VEA) of 4.31 eV, indicating an electronically robust structure [119]. The NICS computations show the $\sigma + \pi$ double aromaticity in the CB_5S_5^+ cluster.

All the above-mentioned global and/or local minimum structures contain one ppC. In 2005, Schleyer and coworkers reported certain fluxional wheel-like species, namely, C_2B_8 , $\text{C}_3\text{B}_9^{3+}$, and $\text{C}_5\text{B}_{11}^+$, in which the interior C_2 , C_3 , and C_5 fragments revolve within the boron rings, respectively (Figure 27) [120]. In C_2B_8 , $\text{C}_3\text{B}_9^{3+}$, and $\text{C}_5\text{B}_{11}^+$ species, there are two, three, and five ppC centers that coexist in the energy minimum geometries, respectively. The NICS computations predict the π -aromaticity of these species with more than one ppC atom. These unusual planar clusters are stable when the constituent elements are suited nicely, both geometrically and electronically.

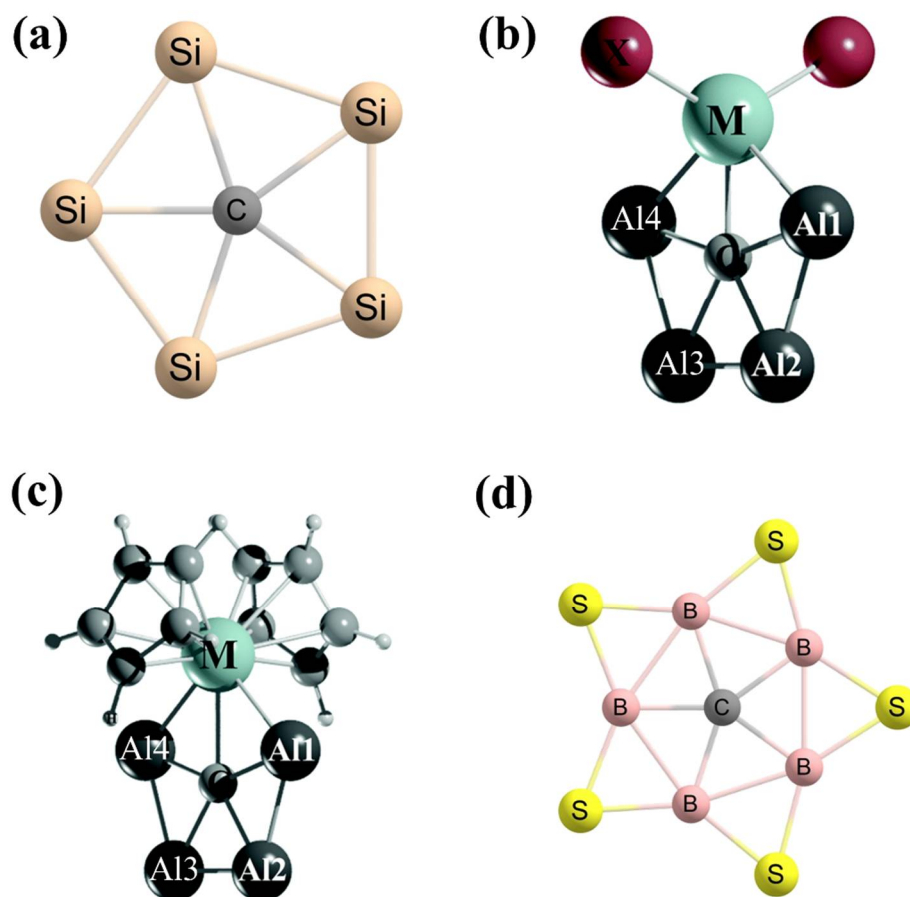


Figure 26. (a) The symmetric structures Si_5C^{2-} and Si_5C^- clusters are ppC species. The monoanionic and dianionic forms have the same shape but different bond lengths. The lowest-energy isomers of (b) CAI_4MX_2 clusters and (c) $\text{CAI}_4\text{M}(\text{C}_5\text{H}_5)_2$ clusters. The global minimum structure of (d) CB_5S_5^+ cluster with a ppC.

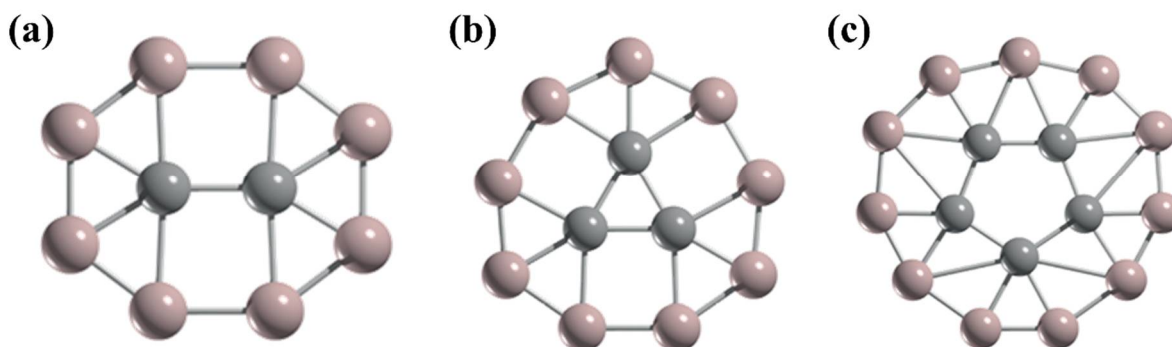


Figure 27. The boron–carbon clusters (a) C_2B_8 , (b) $\text{C}_3\text{B}_9^{3+}$, and (c) $\text{C}_5\text{B}_{11}^+$ are local minimum structures that include conformationally dynamic C_2 , C_3 , and C_5 units, respectively, within boron rings.

4. Planar Hexacoordinate Carbons (phCs)

The possibility of the ptC and ppC molecules and/or ions are discussed in the previous two sections. Now the question arises of whether it is feasible to obtain a planar hexacoordinate carbon (phC) or a planar heptacoordinate carbon, or a planar octacoordinate carbon. In the case of the main group of components, the existence of planar hexacoordination is limited. Despite various species with hexacoordinate carbon being described, they have 3D geometries (Figure 28) [121–123]. In 2000, the first example with a phC is the CB_6^{2-} di-anionic system (Figure 29a), studied by Exner et al. using DFT and high-level ab initio

calculations [124]. This system has a D_{6h} point group of symmetry. The reported structure is not the lowest-energy isomer, rather it is a local minimum with $143.9 \text{ kJ mol}^{-1}$ more energy compared to the lowest-energy structure. This cluster shows benzene-like HOMOs and is aromatic in nature. Figure 30 contains the proposed phC species by Ito et al. utilizing CB_6^{2-} as the building block [125].

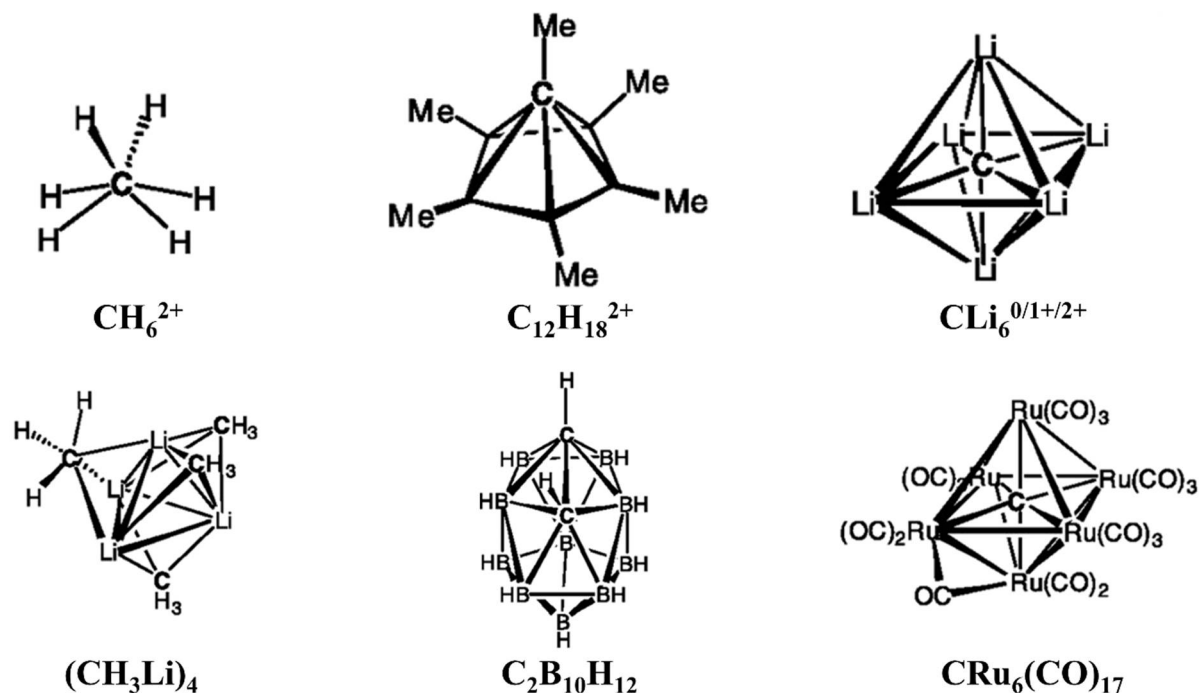


Figure 28. Some compounds with hexacoordinate carbons have three-dimensional structures.

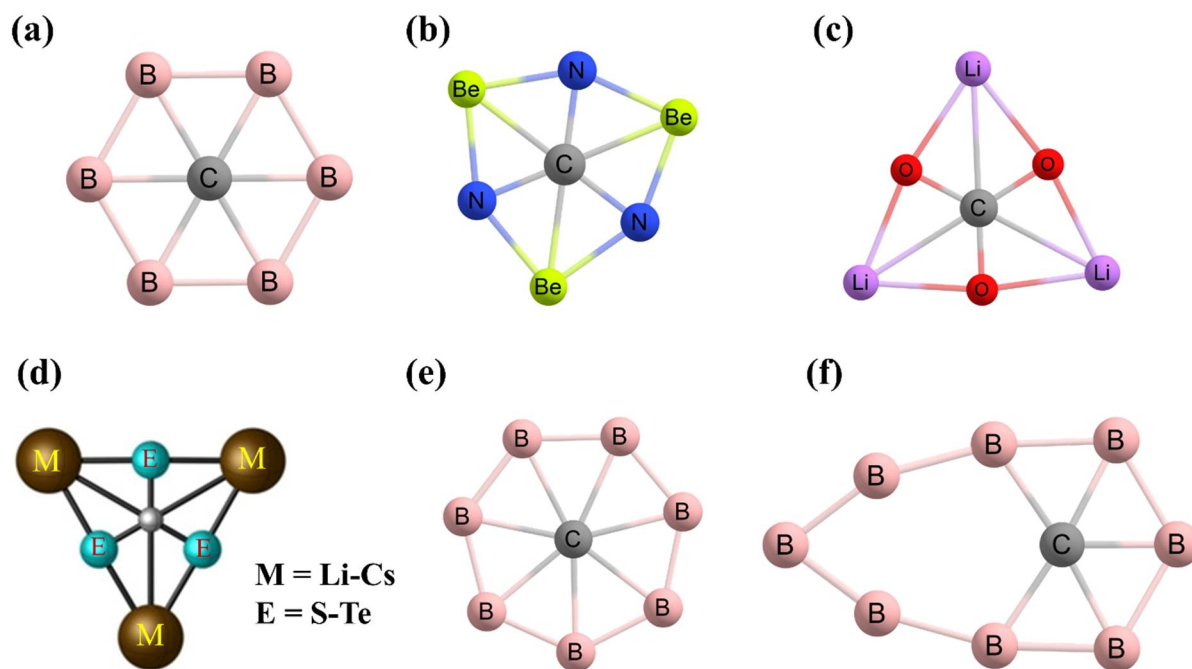


Figure 29. Local minimum structures of (a) CB_6^{2-} and (b) CN_3Be_3^+ clusters with a phC. Global minimum structures of (c) CO_3Li_3^+ and (d) CE_3M_3^+ (E = S-Te, and M = Li-Cs) clusters. Local minimum structures of (e) CB_7^- cluster with planar heptacoordinate carbon. Minimum energy structure of (f) CB_8 cluster with a ppC.

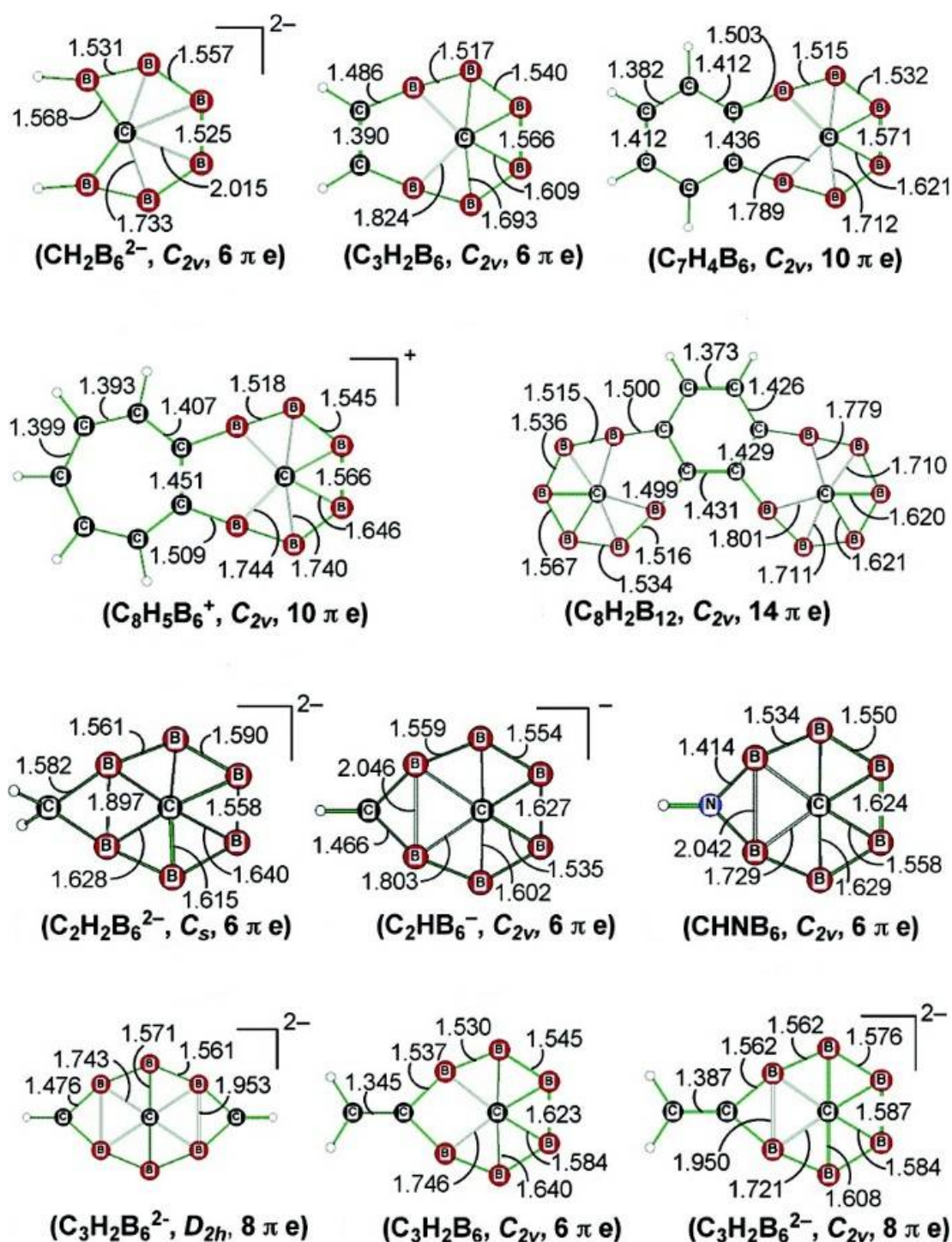


Figure 30. Examples of CB_6^{2-} based phC molecules. Bond lengths are shown in Å. Reprinted from ref. [125] with permission from American Chemical Society. Copyright © 2022 American Chemical Society.

In 2012, Wu et al. used a CB_6^{2-} unit and executed isoelectronic replacement on it to compose unipositive $CN_3Be_3^+$ and $CO_3Li_3^+$ clusters (Figure 29b and 29c, respectively) [126]. Both clusters in their phC structures correspond to the D_{3h} symmetry. The $CN_3Be_3^+$ cluster is a local minimum with 25.5 kJ mol^{-1} more energy with respect to the global minimum geometry. However, the $CO_3Li_3^+$ cluster is a putative global minimum with a phC center. The authors mentioned that the three bridging Li^+ ions stabilized the CO_3^{2-}

ion electrostatically. Later, Leyva-Parra et al. studied the charges on the middle carbon and the bridging Li centers, and the values are 0.87 |e| and 0.97 |e|, respectively [127]. Hence, the positive charges on both carbon and lithium atoms imply electrostatic repulsion between them. Due to this repulsion and the nonappearance of any remarkable orbital overlap between them, this hexacoordinate environment is ambiguous. Because of the different electronegativity values of carbon and oxygen atoms, positive charges on the phC are expected. Therefore, Leyva-Parra et al. substituted the oxygen atoms with the least electronegative sulphur atoms to obtain a true phC atom in the global minimum structures [127]. The fifteen possible $CE_3M_3^+$ (E=S–Te, and M=Li–Cs) combinations are to be identified as phC clusters (Figure 29d). The natural charge analysis shows negative charges on the phC and positive charges on the bridging metal atoms suggesting electrostatic attractions between the partially negative central carbon atom and partially positive bridged metal atoms. These phC clusters were designed following the so-called “*proper polarization of ligand*” approach [127]. Through systematic bonding analyses, the authors stated the covalent nature of the C–E bonds and the ionic nature of the C–M bonds.

5. Higher Coordinate Carbons

The exploration for planar hypercoordinate carbon is not restricted to phC species. Boron rings are broadly utilized to generate planar hypercoordinate carbon species, but the size of the carbon is pivotal for producing the planar structures. For the first time, Minyaev et al. proposed the B_7C^- cluster with a planar heptacoordinate carbon in the local minimum D_{7h} structure (Figure 29e) [128] with 63.9 kcal mol⁻¹ higher energy than the corresponding lowest-energy planar heptacoordinate boron isomer. The authors stated that the B_7C^- system can be considered a substitute for the central B^- ion with a carbon atom in the B_8^{2-} cluster, which contains a heptacoordinate boron atom in the lowest-energy isomer [129]. The magnificent agreement between the experiment and the theory predicted the C_{2v} symmetric global minimum with planar heptacoordinate boron for the B_7C^- system. Hence, from this combined study, the authors concluded that the appearance of the heptacoordinate carbon in the carbon and boron clusters is exceptionally unfavorable. It is hoped that a planar octacoordinate carbon structure will be generated by placing carbon at the center of the B_8 ring. Unfortunately, the smaller size of carbon is the factor that prevents octacoordination in this system. Hence, the planar D_{8h} structure of the B_8C cluster is in a transition state and is converted to a stable ppC cluster with C_{2v} geometry (Figure 29f).

6. Conclusions

This present review documented the recent advancement in the planar hypercoordinate carbon species. These species disobey the primary and most broadly utilized structural rules in organic chemistry and biochemistry. The ttC model proposed by van't Hoff and Le Bel are disobeyed by the theoretically designed and/or experimentally characterized planar orientations of four or more groups in a carbon. These species might have numerous main-group elements and transition-metal atoms as the surrounding ligand atoms. The proposed electronic and mechanical strategies are helpful in designing the ptC compounds. Moreover, the 18-valence electron rule can guide the design of new ptC clusters theoretically as well as experimentally. The formation of three σ and one π bonds among the middle carbon and the surrounding atoms are the consequences of 18-valence electrons. However, the counting of 18-valence electrons is not a prerequisite to have a ptC in a cluster. Various species are described in this review article, in which the 18-valence electrons counting is not followed. Furthermore, this ptC idea is expanded to the probability of a greater coordination number of carbon in planar orientations. Unfortunately, until now, there has been no such logical approach to design ppC, phC, or higher-coordinate carbon molecules/ions.

The experimental validation of the computationally designed planar hypercoordinate carbon molecules/ions is difficult. The species can be feasible in the gas phase if they show enough thermodynamic stability, and interestingly, some ptC species were detected in the

gas phase. All planar hypercoordinate carbon species in the global minima may be feasible in the gas phase. These unusual clusters provide unique properties and have opened new vistas in the allied research fields.

Author Contributions: Conceptualization, P.D.; methodology, P.D. and P.K.C.; software, P.D.; validation, P.D. and P.K.C.; formal analysis, P.D.; investigation, P.D.; resources, P.K.C.; data curation, P.D.; writing—original draft preparation, P.D.; writing—review and editing, P.D. and P.K.C.; visualization, P.D. and P.K.C.; supervision, P.K.C.; project administration, P.K.C.; funding acquisition, P.K.C. All authors have read and agreed to the published version of the manuscript.

Funding: This research was funded by Department of Science and Technology (DST), New Delhi, grant number SR/S2/JCB-09/2009.

Institutional Review Board Statement: Not applicable.

Informed Consent Statement: Not applicable.

Data Availability Statement: Data is contained within the article.

Acknowledgments: PKC thanks Venkatesan Thimmakondlu Samy for the kind invitation to contribute an article to this special collection of articles in “Chemistry” entitled “Hypercoordinate Carbon”. PD and PKC acknowledge all authors and co-authors whose works are documented and presented in this review. PD thanks UGC, New Delhi, India for the Research Fellowship. PKC acknowledges DST, New Delhi, India for the J. C. Bose National Fellowship (grant number SR/S2/JCB-09/2009).

Conflicts of Interest: The authors declare no conflict of interest.

References

1. Bartlett, P.D. *Nonclassical Ions*; WA Benjamin: New York, NY, USA, 1965.
2. Brown, H.C. *The Nonclassical-Ion Problem*; Plenum: New York, NY, USA, 1977.
3. Le-Bel, J.A. On the Relations Which Exist between the Atomic Formulas of Organic Compounds and the Rotatory Power of Their Solutions. *Bull. Soc. Chim. Fr.* **1874**, *22*, 337–347.
4. Minkin, V.I.; Minyaev, R.M.; Hoffmann, R. Nonclassical structures of organic compounds: Non-standard stereochemistry and hypercoordination. *Russ. Chem. Rev.* **2002**, *71*, 869–892. [[CrossRef](#)]
5. Minkin, V.I.; Minyaev, R.M.; Zdanov, J.A. *Nonclassical Structures of Organic Compounds*; Mir: Moscow, Russia, 1987.
6. Das, P.; Pan, S.; Chattaraj, P.K. Planar Hypercoordinate Carbon. In *Atomic Clusters with Unusual Structure, Bonding and Reactivity*; Elsevier: Amsterdam, The Netherlands, 2023; pp. 357–372. [[CrossRef](#)]
7. Yang, L.M.; Ganz, E.; Chen, Z.; Wang, Z.X.; Schleyer, P.V.R. Four decades of the chemistry of planar hypercoordinate compounds. *Angew. Chem. Int. Ed.* **2015**, *54*, 9468–9501. [[CrossRef](#)] [[PubMed](#)]
8. van't Hoff, J.H. A Suggestion Looking to the Extension into Space of the Structural Formulas at Present Used in Chemistry, and a Note upon the Relation between the Optical Activity and the Chemical Constitution of Organic Compounds. *Arch. Neerl. Sci. Exactes Nat.* **1874**, *9*, 445–454.
9. Monkhurst, H.J. Activation Energy for Interconversion of Enantiomers Containing an Asymmetric Carbon Atom without Breaking Bonds. *Chem. Commun.* **1968**, *11*, 1111–1112. [[CrossRef](#)]
10. Wynberg, H.; Hekkert, G.L.; Houbiers, J.P.M.; Bosch, H.W. The Optical Activity of Butylethylhexylpropylmethane. *J. Am. Chem. Soc.* **1965**, *87*, 2635–2639. [[CrossRef](#)]
11. Hoffmann, R.; Alder, R.W.; Wilcox, C.F. Planar Tetracoordinate Carbon. *J. Am. Chem. Soc.* **1970**, *92*, 4992–4993. [[CrossRef](#)]
12. Pepper, M.J.; Shavitt, I.; Schleyer, P.V.R.; Glukhovtsev, M.N.; Janoschek, R.; Quack, M. Is the stereomutation of methane possible? *J. Comput. Chem.* **1995**, *16*, 207–225. [[CrossRef](#)]
13. Golden, D.M.; Walsh, R.; Benson, S.W. The Thermochemistry of the Gas Phase Equilibrium $I_2 + CH_4$ [UNK] $CH_3I + HI$ and the Heat of Formation of the Methyl Radical. *J. Am. Chem. Soc.* **1965**, *87*, 4053–4057. [[CrossRef](#)]
14. Crans, D.C.; Snyder, J.P. Tetracoordinate planar carbon: A singlet biradical. *J. Am. Chem. Soc.* **1980**, *102*, 7152–7154. [[CrossRef](#)]
15. Schleyer, P.V.R.; Boldyrev, A.I. A new, general strategy for achieving planar tetracoordinate geometries for carbon and other second row periodic elements. *J. Chem. Soc. Chem. Commun.* **1991**, 1536–1538. [[CrossRef](#)]
16. Boldyrev, A.I.; Simons, J. Tetracoordinated Planar Carbon in Pentaatomic Molecules. *J. Am. Chem. Soc.* **1998**, *120*, 7967–7972. [[CrossRef](#)]
17. Gribanova, T.N.; Minyaev, R.M.; Minkin, V.I. Planar Tetracoordinate Carbon in Organoboron Compounds: Ab initio Computational Study. *Collect. Czech. Chem. Commun.* **1999**, *64*, 1780–1789. [[CrossRef](#)]
18. Li, X.; Wang, L.S.; Boldyrev, A.I.; Simons, J. Tetracoordinated Planar Carbon in the Al_4C^- Anion. A Combined Photoelectron Spectroscopy and ab Initio Study. *J. Am. Chem. Soc.* **1999**, *121*, 6033–6038. [[CrossRef](#)]

19. Wang, Z.X.; Manojkumar, T.K.; Wannere, C.; Schleyer, P.V.R. A Theoretical Prediction of Potentially Observable Lithium Compounds with Planar Tetracoordinate Carbons. *Org. Lett.* **2001**, *3*, 1249–1252. [[CrossRef](#)]
20. Wang, Z.X.; Schleyer, P.V.R. A New Strategy To Achieve Perfectly Planar Carbon Tetracoordination. *J. Am. Chem. Soc.* **2001**, *123*, 994–995. [[CrossRef](#)]
21. Merino, G.; Méndez-Rojas, M.A.; Vela, A. $(C_5M_{2-n})^{n-}$ ($M = Li, Na, K$, and $n = 0, 1, 2$). A New Family of Molecules Containing Planar Tetracoordinate Carbons. *J. Am. Chem. Soc.* **2003**, *125*, 6026–6027. [[CrossRef](#)]
22. Sahin, Y.; Prasang, C.; Hofmann, M.; Subramanian, G.; Geiseler, G.; Massa, W.; Berndt, A. A Diboracyclopropane with a Planar-Tetracoordinate Carbon Atom and a Triborabicyclobutane. *Angew. Chem. Int. Ed.* **2003**, *42*, 671–674. [[CrossRef](#)]
23. Li, S.D.; Ren, G.M.; Miao, C.Q.; Jin, Z.H. M_4H_4X : Hydrometals ($M = Cu, Ni$) Containing Tetracoordinate Planar Nonmetals ($X = B, C, N, O$). *Angew. Chem. Int. Ed.* **2004**, *43*, 1371–1373. [[CrossRef](#)]
24. Merino, G.; Méndez-Rojas, M.A.; Beltran, H.I.; Corminboeuf, C.; Heine, T.; Vela, A. Theoretical Analysis of the Smallest Carbon Cluster Containing a Planar Tetracoordinate Carbon. *J. Am. Chem. Soc.* **2004**, *126*, 16160–16169. [[CrossRef](#)]
25. Pancharatna, P.D.; Méndez-Rojas, M.A.; Merino, G.; Vela, A.; Hoffmann, R. Planar Tetracoordinate Carbon in Extended Systems. *J. Am. Chem. Soc.* **2004**, *126*, 15309–15315. [[CrossRef](#)] [[PubMed](#)]
26. Priyakumar, U.D.; Reddy, A.S.; Sastry, G.N. The design of molecules containing planar tetracoordinate carbon. *Tetrahedron Lett.* **2004**, *45*, 2495–2498. [[CrossRef](#)]
27. Merino, G.; Méndez-Rojas, M.A.; Vela, A.; Heine, T. Recent advances in planar tetracoordinate carbon chemistry. *J. Comput. Chem.* **2007**, *28*, 362–372. [[CrossRef](#)]
28. Minkin, V.I.; Gribanova, T.N.; Minkin, V.I.; Starikov, A.G.; Hoffmann, R. Planar and Pyramidal Tetracoordinate Carbon in Organoboron Compounds. *J. Org. Chem.* **2005**, *70*, 6693–6704.
29. Su, M.D. Theoretical Designs for Planar Tetracoordinated Carbon in Cu, Ag, and Au Organometallic Chemistry: A New Target for Synthesis. *Inorg. Chem.* **2005**, *44*, 4829–4833. [[CrossRef](#)] [[PubMed](#)]
30. Li, S.D.; Ren, G.M.; Miao, C.Q. $(M_4H_3X)_2B_2O_2$: Hydrometal Complexes ($M = Ni, Mg$) Containing Double Tetracoordinate Planar Nonmetal Centers ($X = C, N$). *J. Phys. Chem. A* **2005**, *109*, 259–261. [[CrossRef](#)] [[PubMed](#)]
31. Esteves, P.M.; Ferreira, N.B.P.; Corrêa, R.J. Neutral Structures with a Planar Tetracoordinated Carbon Based on Spiropentadiene Analogues. *J. Am. Chem. Soc.* **2005**, *127*, 8680–8685. [[CrossRef](#)]
32. Erker, G. Stereochemistry and catalysis with zirconium complexes. *Pure Appl. Chem.* **1991**, *63*, 797–806. [[CrossRef](#)]
33. Erker, G.; Albrecht, M.; Kruger, C.; Werner, S. Novel synthetic route to hydrocarbyl-bridged dinuclear zirconium/aluminum complexes exhibiting a planar tetracoordinate carbon center. *Organometallics* **1991**, *10*, 3791–3793. [[CrossRef](#)]
34. Albrecht, M.; Erker, G.; Nolte, M.; Kruger, C. Planar tetracoordinate carbon stabilized in a dimetallic hafnium/aluminum compound: Formation and crystal structure of $Cp_2Hf[\mu-\eta^1-\eta^2-MeCC(C_6H_{11})][\mu-CC(C_6H_{11})]AlMe_2$. *J. Organomet. Chem.* **1992**, *427*, C21–C25. [[CrossRef](#)]
35. Rottger, D.; Erker, G.; Frohlich, R.; Grehl, M.; Silverio, S.J.; Hylakryspin, I.; Gleiter, R. Determination of the Stabilization Energy of Planar-Tetracoordinate Carbon in Dynamic Dinuclear (μ -Hydrocarbyl)bis(zirconocene) Cation Complexes and Detection of an Organometallic Memory Effect in Their Formation. *J. Am. Chem. Soc.* **1995**, *117*, 10503–10512. [[CrossRef](#)]
36. Rottger, D.; Erker, G.; Frohlich, R. Formation of stable organometallic planar-tetracoordinate carbon compounds containing a cationic ($\mu-R^1CCR^2$) [μ -chloro($ZrCp_2$) $_2$] framework. *J. Organomet. Chem.* **1996**, *518*, 221–225. [[CrossRef](#)]
37. Rottger, D.; Erker, G.; Frohlich, R.; Kotila, S. Stabilization of a Planar-tetracoordinate Carbon Center in an Organometallic Complex Containing Both a Zirconocene and a Hafnocene Moiety. *Chem. Ber.* **1996**, *129*, 1–3. [[CrossRef](#)]
38. Schottek, J.; Erker, G.; Frohlich, R. Formation of Metallocene-Stabilized Planar-Tetracoordinate Carbon Compounds by a Protonation Route. *Eur. J. Inorg. Chem.* **1998**, *1998*, 551–558. [[CrossRef](#)]
39. Choukroun, R.; Donnadieu, B.; Zhao, J.S.; Cassoux, P.; Lepetit, C.; Silvi, B. Synthesis and Characterization of $[Cp_2V(\mu-\eta^2-\eta^4\text{-butadiyne})ZrCp'_2]$ Heterodimetallic Complexes ($Cp' = C_5H_4t\text{-Bu}, C_5H_4Me$). Formation Mechanism and Theoretical (ELF) Evidence for the Existence of Planar Tetracoordinate Carbon (ptC). *Organometallics* **2000**, *19*, 1901–1911. [[CrossRef](#)]
40. Li, X.; Zhang, H.F.; Wang, L.S.; Geske, G.D.; Boldyrev, A.I. Pentaatomic Tetracoordinate Planar Carbon, $[CAI_4]^{2-}$: A New Structural Unit and Its Salt Complexes. *Angew. Chem. Int. Ed.* **2000**, *39*, 3630–3632. [[CrossRef](#)]
41. Hoffmann, R. The theoretical design of novel stabilized systems. *Pure Appl. Chem.* **1971**, *28*, 181–194. [[CrossRef](#)]
42. Sorger, K.; Schleyer, P.V.R. Planar and inherently non-tetrahedral tetracoordinate carbon: A status report. *J. Mol. Struct. THEOCHEM* **1995**, *338*, 317–346. [[CrossRef](#)]
43. Röttger, D.; Erker, G. Compounds containing planar-tetracoordinate carbon. *Angew. Chem. Int. Ed.* **1997**, *36*, 812–827. [[CrossRef](#)]
44. Radom, L.; Rasmussen, D.R. The planar carbon story. *Pure Appl. Chem.* **1998**, *70*, 1977–1984. [[CrossRef](#)]
45. Erker, G. Using bent metallocenes for stabilizing unusual coordination geometries at carbon. *Chem. Soc. Rev.* **1999**, *28*, 307–314. [[CrossRef](#)]
46. Siebert, W.; Gunale, A. Compounds containing a planar-tetracoordinate carbon atom as analogues of planar methane. *Chem. Soc. Rev.* **1999**, *28*, 367–371. [[CrossRef](#)]
47. Keese, R. Carbon flatland: planar tetracoordinate carbon and fenestrenes. *Chem. Rev.* **2006**, *106*, 4787–4808. [[CrossRef](#)]
48. McGrath, M.P.; Radom, L. Alkapanes: A class of neutral hydrocarbons containing a potentially planar tetracoordinate carbon. *J. Am. Chem. Soc.* **1993**, *115*, 3320–3321. [[CrossRef](#)]

49. Lyons, J.E.; Rasmussen, D.R.; McGrath, M.P.; Nobes, R.H.; Radom, L. Octaplan: Ein gesättigter Kohlenwasserstoff mit ungewöhnlich niedriger Ionisierungsenergie und einem planar-tetrakoordinierten Kohlenstoffatom im Radikalkation. *Angew. Chem. Int. Ed. Engl.* **1994**, *33*, 1667–1668. [[CrossRef](#)]
50. Ding, B.W.; Keese, R.; Stoeckli-Evans, H. First Synthesis and Structure of a Tetraazasilafenestrane. *Angew. Chem. Int. Ed.* **1999**, *38*, 375–376. [[CrossRef](#)]
51. Rasmussen, D.R.; Radom, L. Planar tetrakoordinierter Kohlenstoff in einem neutralen gesättigten Kohlenwasserstoff: Theoretischer Entwurf und Charakterisierung. *Angew. Chem. Int. Ed.* **1999**, *38*, 2875–2878. [[CrossRef](#)]
52. Wang, Z.X.; Schleyer, P.v.R. The Theoretical Design of Neutral Planar Tetracoordinate Carbon Molecules with C(C)₄ Substructures. *J. Am. Chem. Soc.* **2002**, *124*, 11979–11982. [[CrossRef](#)]
53. Collins, J.B.; Dill, J.D.; Jemmis, E.D.; Apeloig, Y.; Schleyer, P.v.R.; Seeger, R.; Pople, J.A. Stabilization of Planar Tetracoordinate Carbon. *J. Am. Chem. Soc.* **1976**, *98*, 5419–5427. [[CrossRef](#)]
54. Cotton, F.A.; Millar, M. The probable existence of a triple bond between two vanadium atoms. *J. Am. Chem. Soc.* **1977**, *99*, 7886–7891. [[CrossRef](#)]
55. Xie, Y.; Schaefer, H.F. Hexalithiobenzene: A *D*_{6h} equilibrium geometry with six lithium atoms in bridging positions. *Chem. Phys. Lett.* **1991**, *179*, 563–567. [[CrossRef](#)]
56. Wang, L.S.; Boldyrev, A.I.; Li, X.; Simons, J. Experimental Observation of Pentaatomic Tetracoordinate Planar Carbon-Containing Molecules. *J. Am. Chem. Soc.* **2000**, *122*, 7681–7687. [[CrossRef](#)]
57. Castro, A.C.; Audiffred, M.; Mercero, J.M.; Ugalde, J.M.; Méndez-Rojas, M.A.; Merino, G. Planar tetracoordinate carbon in CE₄²⁻ (E = Al–Tl) clusters. *Chem. Phys. Lett.* **2012**, *519–520*, 29–33. [[CrossRef](#)]
58. Cui, Z.H.; Ding, Y.H.; Cabellos, J.L.; Osorio, E.; Islas, R.; Restrepo, A.; Merino, G. Planar tetracoordinate carbons with a double bond in CA₃E clusters. *Phys. Chem. Chem. Phys.* **2015**, *17*, 8769–8775. [[CrossRef](#)]
59. Chakraborty, D.; Chattaraj, P.K. Conceptual Density Functional Theory based Electronic Structure Principles. *Chem. Sci.* **2021**, *12*, 6264–6279. [[CrossRef](#)]
60. Chattaraj, P.K.; Cedillo, A.; Parr, R.G.; Arnett, E.M. Appraisal of Chemical Bond Making, Bond Breaking, and Electron Transfer in Solution in the Light of the Principle of Maximum Hardness. *J. Org. Chem.* **1995**, *60*, 4707–4714. [[CrossRef](#)]
61. Parr, R.G.; Chattaraj, P.K. Principle of maximum hardness. *J. Am. Chem. Soc.* **1991**, *113*, 1854–1855. [[CrossRef](#)]
62. Wiberg, K.B. Application of the pople-santry-segal CNDO method to the cyclopropylcarbinyl and cyclobutyl cation and to bicyclobutane. *Tetrahedron* **1968**, *24*, 1083–1096. [[CrossRef](#)]
63. Zubarev, D.Y.; Boldyrev, A.I. Developing Paradigms of Chemical Bonding: Adaptive Natural Density Partitioning. *Phys. Chem. Chem. Phys.* **2008**, *10*, 5207–5217. [[CrossRef](#)]
64. Zubarev, D.Y.; Boldyrev, A.I. Revealing Intuitively Assessable Chemical Bonding Patterns in Organic Aromatic Molecules via Adaptive Natural Density Partitioning. *J. Org. Chem.* **2008**, *73*, 9251–9258. [[CrossRef](#)]
65. Millam, J.M.; Bakken, V.; Chen, W.; Hase, W.L.; Schlegel, H.B. Ab initio classical trajectories on the Born–Oppenheimer surface: Hessian-based integrators using fifth-order polynomial and rational function fits. *J. Chem. Phys.* **1999**, *111*, 3800–3805. [[CrossRef](#)]
66. Job, N.; Khatun, M.; Thirumoorthy, K.; CH, S.S.R.; Chandrasekaran, V.; Anoop, A.; Thimmakondur, V.S. CA₄Mg^{0/−}: Global Minima with a Planar Tetracoordinate Carbon Atom. *Atoms* **2021**, *9*, 24. [[CrossRef](#)]
67. Schleyer, P.v.R.; Maerker, C.; Dransfeld, A.; Jiao, H.; Hommes, M.J.R.V.E. Nucleus-Independent Chemical Shifts: A Simple and Efficient Aromaticity Probe. *J. Am. Chem. Soc.* **1996**, *118*, 6317–6318. [[CrossRef](#)] [[PubMed](#)]
68. Das, P.; Patra, S.G.; Chattaraj, P.K. CB₆Al^{0/+}: Planar hexacoordinate boron (phB) in the global minimum structure. *Phys. Chem. Chem. Phys.* **2022**, *24*, 22634–22644. [[CrossRef](#)] [[PubMed](#)]
69. Das, P.; Chattaraj, P.K. Electride characteristics of some binuclear sandwich complexes of alkaline earth metals, M₂(η⁵-L)₂ (M = Be, Mg; L = C₅H₅[−], N₅[−], P₅[−], As₅[−]). *J. Phys. Chem. A* **2020**, *124*, 9801–9810. [[CrossRef](#)] [[PubMed](#)]
70. Das, P.; Chattaraj, P.K. Substituent effects on electride characteristics of Mg₂(η⁵-C₅H₅)₂: A theoretical study. *J. Phys. Chem. A* **2021**, *125*, 6207–6220. [[CrossRef](#)]
71. Schlegel, H.B.; Millam, J.M.; Iyengar, S.S.; Voth, G.A.; Daniels, A.D.; Scuseria, G.E.; Frisch, M.J. Ab initio molecular dynamics: Propagating the density matrix with Gaussian orbitals. *J. Chem. Phys.* **2001**, *114*, 9758–9763. [[CrossRef](#)]
72. Iyengar, S.S.; Schlegel, H.B.; Millam, J.M.; Voth, G.A.; Scuseria, G.E.; Frisch, M.J. Ab initio molecular dynamics: Propagating the density matrix with Gaussian orbitals. II. Generalizations based on mass-weighting, idempotency, energy conservation and choice of initial conditions. *J. Chem. Phys.* **2001**, *115*, 10291–10302. [[CrossRef](#)]
73. Schlegel, H.B.; Iyengar, S.S.; Li, X.; Millam, J.M.; Voth, G.A.; Scuseria, G.E.; Frisch, M.J. Ab initio molecular dynamics: Propagating the density matrix with Gaussian orbitals. III. Comparison with Born–Oppenheimer dynamics. *J. Chem. Phys.* **2002**, *117*, 8694–8704. [[CrossRef](#)]
74. Das, P.; Saha, R.; Chattaraj, P.K. Encapsulation of Mg₂ inside a C₆₀ cage forms an electride. *J. Comput. Chem.* **2020**, *41*, 1645–1653. [[CrossRef](#)]
75. Das, P.; Chattaraj, P.K. Comparison Between Electride Characteristics of Li₃@B₄₀ and Li₃@C₆₀. *Front. Chem.* **2021**, *9*, 638581. [[CrossRef](#)] [[PubMed](#)]
76. Savin, A.; Nesper, R.; Wengert, S.; Fässler, T.F. ELF: The Electron Localization Function. *Angew. Chem. Int. Ed.* **1997**, *36*, 1808–1832. [[CrossRef](#)]

77. Saha, R.; Das, P.; Chattaraj, P.K. Molecular Electrides: An In Silico Perspective. *ChemPhysChem* **2022**, *23*, e202200329. [[CrossRef](#)] [[PubMed](#)]
78. Das, P.; Chattaraj, P.K. In Silico Studies on Selected Neutral Molecules, CGa_2Ge_2 , CALGaGe_2 , and CSiGa_2Ge Containing Planar Tetracoordinate Carbon. *Atoms* **2021**, *9*, 65. [[CrossRef](#)]
79. Das, P.; Chattaraj, P.K. $\text{CSiGaAl}_2^{-/0}$ and $\text{CGeGaAl}_2^{-/0}$ having planar tetracoordinate carbon atoms in their global minimum energy structures. *J. Comput. Chem.* **2022**, *43*, 894–905. [[CrossRef](#)]
80. Das, P.; Khatun, M.; Anoop, A.; Chattaraj, P.K. $\text{CSi}_n\text{Ge}_{4-n}^{2+}$ ($n = 1-3$): Prospective systems containing planar tetracoordinate carbon (ptC). *Phys. Chem. Chem. Phys.* **2022**, *24*, 16701–16711. [[CrossRef](#)]
81. Zhang, J.; Dolg, M. ABCluster: The artificial bee colony algorithm for cluster global optimization. *Phys. Chem. Chem. Phys.* **2015**, *17*, 24173–24181. [[CrossRef](#)]
82. Zhang, J.; Dolg, M. Global optimization of clusters of rigid molecules using the artificial bee colony algorithm. *Phys. Chem. Chem. Phys.* **2016**, *18*, 3003–3010. [[CrossRef](#)]
83. Karaboga, D. *An Idea Based on Honey Bee Swarm for Numerical Optimization, Technical Report-TR06*; Erciyes University, Engineering Faculty, Computer Engineering Department: Kayseri, Türkiye, 2005.
84. Sarkar, K.; Bhattacharyya, S.P. *Soft Computing in Chemical and Physical Sciences: A Shift in Computing Paradigm*, 1st ed.; CRC Press: Boca Raton, FL, USA, 2017. [[CrossRef](#)]
85. Cui, Z.H.; Contreras, M.; Ding, Y.H.; Merino, G. Planar Tetracoordinate Carbon versus Planar Tetracoordinate Boron: The Case of CB_4 and Its Cation. *J. Am. Chem. Soc.* **2011**, *133*, 13228–13231. [[CrossRef](#)]
86. Becker, S.; Dietze, H.J. Cluster ions in the laser mass spectra of boron carbide. *Int. J. Mass Spectrom. Ion Process.* **1988**, *82*, 287–298. [[CrossRef](#)]
87. Vogt-Geisse, S.; Wu, J.I.C.; Schleyer, P.v.R.; Schaefer, H.F. Bonding, aromaticity, and planar tetracoordinated carbon in Si_2CH_2 and Ge_2CH_2 . *J. Mol. Model* **2015**, *21*, 217. [[CrossRef](#)] [[PubMed](#)]
88. Guo, J.Y.; Chai, H.Y.; Duan, Q.; Qin, J.M.; Shen, X.D.; Jiang, D.Y.; Hou, J.H.; Yan, B.; Li, Z.R.; Gu, F.L.; et al. Planar tetracoordinate carbon species CLi_3E with 12-valence-electrons. *Phys. Chem. Chem. Phys.* **2016**, *18*, 4589–4593. [[CrossRef](#)]
89. Das, P.; Chattaraj, P.K. Electride characteristics of $\text{M}_2(\eta^5\text{-E}_5)_2$ ($\text{M} = \text{Be, Mg; E} = \text{Sb}_5^-$). *Struct. Chem.* **2021**, *32*, 2107–2114. [[CrossRef](#)]
90. Das, P.; Chattaraj, P.K. Stabilisation of Li(0)-Li(0) bond by normal and mesoionic carbenes and electride characteristics of the complexes. *Mol. Phys.* **2022**, *120*, e2026512. [[CrossRef](#)]
91. Zheng, H.F.; Yu, S.; Hu, T.D.; Xu, J.; Ding, Y.H. CAL_3X ($\text{X} = \text{B/Al/Ga/In/Tl}$) with 16 Valence Electrons: Can Planar Tetracoordinate Carbon Be Stable? *Phys. Chem. Chem. Phys.* **2018**, *20*, 26266–26272. [[CrossRef](#)]
92. Ravell, E.; Jalife, S.; Barroso, J.; Orozco-Ic, M.; Hernandez-Juarez, G.; Ortiz-Chi, F.; Pan, S.; Cabellos, J.L.; Merino, G. Structure and Bonding in CE_5^- ($\text{E} = \text{Al - Tl}$) Clusters: Planar Tetracoordinate Carbon vs Pentacoordinate Carbon. *Chem.-Asian J.* **2018**, *13*, 1467–1473. [[CrossRef](#)]
93. Guo, J.C.; Feng, L.Y.; Dong, C.; Zhai, H.J. Ternary 12-electron CBe_3X_3^+ ($\text{X} = \text{H, Li, Na, Cu, Ag}$) Clusters: Planar Tetracoordinate Carbons and Superalkali Cations. *Phys. Chem. Chem. Phys.* **2019**, *21*, 22048–22056. [[CrossRef](#)]
94. Wu, X.F.; Cheng, Y.X.; Guo, J.C. CLiAl_2E and CLi_2AlE ($\text{E} = \text{P, As, Sb, Bi}$): Planar Tetracoordinate Carbon Clusters with 16 and 14 Valence Electrons. *ACS Omega* **2019**, *4*, 21311–21318. [[CrossRef](#)]
95. Leyva-Parra, L.; Diego, L.; Inostroza, D.; Yañez, O.; Pumachagua-Huertas, R.; Barroso, J.; Vásquez-Espinal, A.; Merino, G.; Tiznado, W. Planar Hypercoordinate Carbons in Alkali Metal Decorated CE_3^{2-} and CE_2^{2-} Dianions. *Chem. Eur. J.* **2021**, *27*, 16701–16706. [[CrossRef](#)]
96. Yañez, O.; Vásquez-Espinal, A.; Pino-Rios, R.; Ferraro, F.; Pan, S.; Osorio, E.; Merino, G.; Tiznado, W. Exploiting electronic strategies to stabilize a planar tetracoordinate carbon in cyclic aromatic hydrocarbons. *Chem. Commun.* **2017**, *53*, 12112–12115. [[CrossRef](#)]
97. Wang, M.; Orozco-Ic, M.; Leyva-Parra, L.; Tiznado, W.; Barroso, J.; Ding, Y.; Cui, Z.H.; Merino, G. Planar Tetracoordinate Carbons in Allene-Type Structures. *J. Phys. Chem. A* **2021**, *125*, 3009–3014. [[CrossRef](#)] [[PubMed](#)]
98. Inostroza, D.; Leyva-Parra, L.; Vásquez-Espinal, A.; Contreras-García, J.; Cui, Z.H.; Pan, S.; Thimmakonda, V.S.; Tiznado, W. E_6C_{15} ($\text{E} = \text{Si-Pb}$): Polycyclic aromatic compounds with three planar tetracoordinate carbons. *Chem. Commun.* **2022**, *58*, 13075–13078. [[CrossRef](#)] [[PubMed](#)]
99. Xu, J.; Zhang, X.; Yu, S.; Ding, Y.H.; Bowen, K.H. Identifying the Hydrogenated Planar Tetracoordinate Carbon: A Combined Experimental and Theoretical Study of CAL_4H and CAL_4H^- . *J. Phys. Chem. Lett.* **2017**, *8*, 2263–2267. [[CrossRef](#)] [[PubMed](#)]
100. Vassilev-Galindo, V.; Pan, S.; Donald, K.J.; Merino, G. Planar pentacoordinate carbons. *Nat. Rev. Chem.* **2018**, *2*, 0114. [[CrossRef](#)]
101. Bolton, E.E.; Laidig, W.D.; Schleyer, P.v.R.; Schaefer, H.F. Does singlet 1,1-dithioethene really prefer a perpendicular structure? *J. Phys. Chem.* **1995**, *99*, 17551–17557. [[CrossRef](#)]
102. Wang, Z.X.; Schleyer, P.v.R. Construction principles of “hyparenes”: Families of molecules with planar pentacoordinate carbons. *Science* **2001**, *292*, 2465–2469. [[CrossRef](#)]
103. Tsipis, C.A.; Karagiannis, E.E.; Kladou, P.F.; Tsipis, A.C. Aromatic Gold and Silver ‘Rings’: Hydrosilver(I) and Hydrogold(I) Analogues of Aromatic Hydrocarbons. *J. Am. Chem. Soc.* **2004**, *126*, 12916–12929. [[CrossRef](#)]
104. Tsipis, A.C.; Tsipis, C.A. Hydrometal Analogues of Aromatic Hydrocarbons: A New Class of Cyclic Hydrocoppers(I). *J. Am. Chem. Soc.* **2003**, *125*, 1136–1137. [[CrossRef](#)]

105. Li, S.D.; Miao, C.Q.; Ren, G.M. D_{5h} Cu_5H_5X : Pentagonal hydrocopper Cu_5H_5 containing pentacoordinate planar nonmetal centers ($X = B, C, N, O$). *Eur. J. Inorg. Chem.* **2004**, *2004*, 2232–2234. [[CrossRef](#)]
106. Li, S.D.; Guo, Q.L.; Miao, C.Q.; Ren, G.M. Investigation on transition-metal hydrometal complexes $MnHnC$ with planar coordinate carbon centers by density functional theory. *Acta Phys. Chim. Sin.* **2007**, *23*, 743–745.
107. Pei, Y.; An, W.; Ito, K.; Schleyer, P.v.R.; Zeng, X.C. Planar pentacoordinate carbon in CAI_5^+ : A global minimum. *J. Am. Chem. Soc.* **2008**, *130*, 10394–10400. [[CrossRef](#)] [[PubMed](#)]
108. Jimenez-Halla, J.O.C.; Wu, Y.B.; Wang, Z.X.; Islas, R.; Heine, T.; Merino, G. CAI_4Be and $CAI_3Be_2^-$: Global Minima with a Planar Pentacoordinate Carbon Atom. *Chem. Commun.* **2010**, *46*, 8776–8778. [[CrossRef](#)] [[PubMed](#)]
109. Wu, Y.B.; Duan, Y.; Lu, H.G.; Li, S.D. $CAI_2Be_3^{2-}$ and its salt complex $LiCAI_2Be_3^-$: Anionic global minimum with planar pentacoordinate carbon. *J. Phys. Chem. A* **2012**, *116*, 3290–3294. [[CrossRef](#)] [[PubMed](#)]
110. Castro, A.C.; Martínez-Guajardo, G.; Johnson, T.; Ugalde, J.M.; Wu, Y.B.; Mercero, J.M.; Heine, T.; Donald, K.J.; Merino, G. CBe_5E^- ($E = Al, Ga, In, Tl$): Planar pentacoordinate carbon in heptaatomic clusters. *Phys. Chem. Chem. Phys.* **2012**, *14*, 14764–14768. [[CrossRef](#)]
111. Luo, Q. Theoretical observation of hexaatomic molecules containing pentacoordinate planar carbon. *Sci. China, Ser. B Chem.* **2008**, *51*, 1030–1035. [[CrossRef](#)]
112. Grande-Aztatzi, R.; Cabellos, J.L.; Islas, R.; Infante, I.; Mercero, J.M.; Restrepo, A.; Merino, G. Planar pentacoordinate carbons in CBe_5^{4-} derivatives. *Phys. Chem. Chem. Phys.* **2015**, *17*, 4620–4624. [[CrossRef](#)]
113. Guo, J.C.; Ren, G.M.; Miao, C.Q.; Tian, W.J.; Wu, Y.B.; Wang, X. $CBe_5H_n^{n-4}$ ($n = 2-5$): Hydrogen-stabilized CBe_5 pentagons containing planar or quasi-planar pentacoordinate carbons. *J. Phys. Chem. A* **2015**, *119*, 13101–13106. [[CrossRef](#)]
114. Guo, J.C.; Tian, W.J.; Wang, Y.J.; Zhao, X.F.; Wu, Y.B.; Zhai, H.J.; Li, S.D. Star-like superalkali cations featuring planar pentacoordinate carbon. *J. Chem. Phys.* **2016**, *144*, 244303. [[CrossRef](#)]
115. Zhao, X.F.; Bian, J.H.; Huang, F.; Yuan, C.; Wang, Q.; Liu, P.; Li, D.; Wang, X.; Wu, Y.B. Stabilization of beryllium-containing planar pentacoordinate carbon species through attaching hydrogen atoms. *RSC Adv.* **2018**, *8*, 36521–36526. [[CrossRef](#)]
116. Pan, S.; Cabellos, J.L.; Orozco-Ic, M.; Chattaraj, P.K.; Zhao, L.; Merino, G. Planar pentacoordinate carbon in CGa_5^+ derivatives. *Phys. Chem. Chem. Phys.* **2018**, *20*, 12350–12355. [[CrossRef](#)]
117. Zdetsis, A.D. Novel pentagonal silicon rings and nanowheels stabilized by flat pentacoordinate carbon(s). *J. Chem. Phys.* **2011**, *134*, 094312. [[CrossRef](#)] [[PubMed](#)]
118. Cui, Z.H.; Vassilev-Galindo, V.; Cabellos, J.L.; Osorio, E.; Orozco, M.; Pan, S.; Ding, Y.H.; Merino, G. Planar pentacoordinate carbon atoms embedded in a metallocene framework. *Chem. Commun.* **2017**, *53*, 138–141. [[CrossRef](#)] [[PubMed](#)]
119. Sun, R.; Jin, B.; Huo, B.; Yuan, C.; Zhai, H.J.; Wu, Y.B. Planar pentacoordinate carbon in a sulphur-surrounded boron wheel: The global minimum of $CB_5S_5^+$. *Chem. Commun.* **2022**, *58*, 2552–2555. [[CrossRef](#)] [[PubMed](#)]
120. Erhardt, S.; Frenking, G.; Chen, Z.F.; Schleyer, P.v.R. Aromatic boron wheels with more than one carbon atom in the center: C_2B_8 , $C_3B_9^{3+}$, and $C_5B_{11}^+$. *Angew. Chem. Int. Ed.* **2005**, *44*, 1078–1082. [[CrossRef](#)]
121. Lammertsma, K.; Barzaghi, M.; Olah, G.A.; Pople, J.A.; Schleyer, P.v.R.; Simonetta, M. Carbocations. 7. Structure and stability of diprotonated methane, CH_6^{2+} . *J. Am. Chem. Soc.* **1983**, *105*, 5258–5263. [[CrossRef](#)]
122. Sirigu, A.; Bianchi, M.; Benedetti, E. The crystal structure of $Ru_6C(CO)_{17}$. *J. Chem. Soc. D* **1969**, 596a. [[CrossRef](#)]
123. Hogeveen, H.; Kwant, P.W. Pyramidal mono- and dications. Bridge between organic and organometallic chemistry. *Acc. Chem. Res.* **1975**, *8*, 413–420. [[CrossRef](#)]
124. Exner, K.; Schleyer, P.v.R. Planar Hexacoordinate Carbon: A Viable Possibility. *Science* **2000**, *290*, 1937–1940. [[CrossRef](#)]
125. Ito, K.; Chen, Z.; Corminboeuf, C.; Wannere, C.S.; Zhang, X.H.; Li, Q.S.; Schleyer, P.v.R. Myriad planar hexacoordinate carbon molecules inviting synthesis. *J. Am. Chem. Soc.* **2007**, *129*, 1510–1511. [[CrossRef](#)]
126. Wu, Y.B.; Duan, Y.; Lu, G.; Lu, H.G.; Yang, P.; Schleyer, P.v.R.; Merino, G.; Islas, R.; Wang, Z.X. D_{3h} $CN_3Be_3^+$ and $CO_3Li_3^+$: Viable planar hexacoordinate carbon prototypes. *Phys. Chem. Chem. Phys.* **2012**, *14*, 14760–14763. [[CrossRef](#)]
127. Leyva-Parra, L.; Diego, L.; Yañez, O.; Inostroza, D.; Barroso, J.; Vásquez-Espinal, A.; Merino, G.; Tiznado, W. Planar hexacoordinate carbons: Half covalent, half ionic. *Angew. Chem. Int. Ed.* **2021**, *60*, 8700–8704. [[CrossRef](#)] [[PubMed](#)]
128. Minyaev, R.M.; Gribanova, T.N.; Starikov, A.G.; Minkin, V.I. Heptacoordinated carbon and nitrogen in a planar boron ring. *Dokl. Chem.* **2002**, *382*, 41–45. [[CrossRef](#)]
129. Zhai, H.J.; Alexandrova, A.N.; Birch, K.A.; Boldyrev, A.I.; Wang, L.S. Hepta- and Octacoordinate Boron in Molecular Wheels of Eight- and Nine-Atom Boron Clusters: Observation and Confirmation. *Angew. Chem. Int. Ed.* **2003**, *42*, 6004–6008. [[CrossRef](#)] [[PubMed](#)]